



Vision Guidance System for 6-DoF Robotic Manipulator

Master Thesis

Mechatronics Program

Supervisor: Prof. Mart Tamre

Student: Udith Ajeevan Parthiban
177306 MAHM

E-mail: udpart@ttu.ee

Study program: Mechatronics

Tallinn 2019

AUTHOR'S DECLARATION

Hereby I declare, that I have written this thesis independently.

No academic degree has been applied for based on this material. All works, major viewpoints and data of the other authors used in this thesis have been referenced.

"....." 2019.

Author:
/signature /

Thesis is in accordance with terms and requirements

"....." 2019.

Supervisor:
/signature/

Thesis is in accordance with terms and requirements

"....." 2019.

Co - Supervisor:
/signature/

Accepted for defence

"....."2019.

Chairman of these defense commission:
/name and signature/

DEPARTMENT OF ELECTRICAL POWER ENGINEERING AND MECHATRONICS

THESIS TASK

Student: Udith Ajeevan Parthiban, 177306 MAHM
Study programme, main specialty: MAHM02/13 - Mechatronics
Supervisor: Prof. Mart Tamre
Co - Supervisor: Dr. Salvador Gonzalez Perez

Thesis topic:

(in English) Vision Guidance System for 6-DoF Robotic Manipulator
(in Estonian) Nägemissüsteem 6-e vabadusastmega robotilisele manipulaatorile

Thesis Main Objective

1. Automating thermal material dispensing process.

Thesis tasks and time schedule:

No	Task description	Completion date
1.	Research of previous work	15.01.2019
2.	Formulation of methodology and implementation	02.02.2019
3.	Presentation of results and conclusion of research	25.05.2019

Language of thesis: English

Deadline for submission of thesis: 21.05.2019

Student: Udith Ajeevan Parthiban

Supervisor: Prof. Mart Tamre

Foreword

In English

The revelation for this thesis work comes from the organization's persistent efforts in creating smart manufacturing environment in their production facility. Hence, the inspiration for this project is derived from the author's time in ERICSSON EESTI AS working as an Engineer. All thesis experiments have been performed in the ERICSSON EESTI AS manufacturing facility. The thesis work is dedicated in the field of Machine Vision and Robot Control.

The Author sincerely thanks the supervisors Prof. Mart Tamre and Dr. Salvador Gonzalez Perez for providing every necessary guidance to this thesis work. Author would like to thank Sirli Männiksaar, Head of Operational Efficiency at ERICSSON EESTI AS and Annika Kaseorg, HR Project Manager at ERICSSON EESTI AS for their support and congruency. Further gratitude extended to Production Technology Engineers Ashish Rana and Kaarel Barinov for supporting with the necessary hardware required to run the tests. Alast, Kristina Poolak, who helped in translating the foreword and summary.

In Estonian

Järgneva lõputöö teema tuleneb organisatsiooni püsivatest pingutustest loomaks oma tootmisüksuses tarka tootmiskeskonda. Inspiratsioon järgneva projekti jaoks on saadud autori poolt, ajal, mil ta töötas ERICSSON EESTI AS'is. Kõik lõputöö katsed on teostatud ERICSSON EESTI AS tootmisüksuses. Lõputöö teema on pühendatud kahele valdkonnale: masina nägemisele (Machine Vision) ja roboti juhtimisele (Robot Control).

Autor tänab siiralt juhendajaid Mart Tamret ja Dr.Salvador Gonzalez'i , nemad tagasid kõik vajalikud juhised lõputöö tegemisel. Autor tahab ka tänada Sirli Männiksaart (operatiivtöhususe juht) ja Annika Kaseorgi (inimressurside projektijuht), kes mõlemad töötavad Ericsson Eesti AS'is, nende toetuse ja ühilduvuse eest. Edasised tänusõnad kuuluvad tootmistehnoloogia inseneridele Ashish Ranale ja Kaarel Barinovile, kes toetasid vajaliku riisvaraga testide jaoks. Viimaks, Kristina Poolakut, kes abistas tõlketööga töö eessõnas ja kokkuvõttes.

Contents

Foreword	4
In English.....	4
In Estonian.....	4
List of Figures	7
List of Tables	8
1.Introduction	9
1.1 Motivation.....	10
1.2 Task Objective	10
1.3 Literature Review and Background.....	11
1.3.1 Justification for choosing current implementation.....	12
1.4 Thesis Structure	12
2.Conceptual Design.....	13
2.1 Existing process method	13
2.2 Alternate method Proposal.....	16
3.Mathematical Modelling.....	17
3.1 Vector Solution	17
4.Implementation.....	22
4.1 Hardware Setup.....	22
4.2 Overview of the System	26
5.Inspection	29
5.1 Problem Statement.....	31
5.2 Machine Vision Lighting	32
5.3 Pixel Resolution Calculation	35
5.4 Analysis Tool Precision.....	36
5.5 Automated Optical Inspection.....	38
6.Results.....	39
6.1 Lighting Techniques	39
6.1.1 Conclusion	43
6.2 Automatic Optical Inspection (AOI)	44
6.2.1 Conclusion	46
7.Discussion	47
8.Summary.....	49
8.1 Summary (English)	49
8.2 Summary (Estonian).....	50

Bibliography	51
Appendix.....	53
Appendix A.....	53
Appendix B.....	57

List of Figures

Figure 2.1: Existing Process task in manual mode.....	13
Figure 2.2: Thermal putty dispensing points recommended by Designers.....	14
Figure 2.3: Nordson manual dispensing gun derived from [30]	15
Figure 2.4: Proposed alternate dispensing method with robotic manipulator	16
Figure 3.1: Mathematical Model denoted with various coordinate systems.....	18
Figure 4.1: Overview of the communication setup for camera and robot.....	23
Figure 4.2: Panasonic ME-HGC1000 micro laser sensor derived from [29].....	23
Figure 4.3: Nordson 736HPA-NV pressure dispense valve system derived from [30]	24
Figure 4.4: GRACO Dynamite Extruder derived from [31].....	25
Figure 4.5: Image of the radio surface acquired from SICK PIM60 camera.....	26
Figure 4.6: Introducing geometrical shapes on the obtained image with camera tool	26
Figure 4.7: Initialization of the hardware from the robot controller	27
Figure 4.8: Overview of the system configuration	28
Figure 5.1: Block diagram of a typical vision system from [5]	30
Figure 5.2: Test setup for Automatic Optical Inspection	31
Figure 5.3: Illumination techniques used in Machine Vision derived from [32].....	32
Figure 5.4: Experimental setup for Back Light illumination technique	32
Figure 5.5: Experimental setup for diffused dome light illumination technique.....	33
Figure 5.6: Experimental setup for Ring light illumination technique.....	33
Figure 5.7: Experimental setup for Low angle dark field illumination technique	34
Figure 5.8: Relationship between resolution, precision and accuracy.....	35
Figure 5.9: Image analysis from the Analysis Tool	36
Figure 5.10: Dispensed thermal materials under various control parameters.....	37
Figure 5.11: Observation of good samples and bad samples from the dispensed components	37
Figure 5.12: Expected thermal material quantities with tolerances	38
Figure 6.1: Experimental setup for various lighting conditions	39
Figure 6.2: Image acquired under diffused dome lighting illumination method.....	40
Figure 6.3: Thermal material dimension definition from the camera tool.....	40
Figure 6.4: Image acquired under Brightfield illumination method.....	41
Figure 6.5: Image acquired under low-angle darkfield illumination method	41
Figure 6.6: Image acquired under Backlight illumination method.....	42
Figure 6.7: Comparison between good sample and bad sample observed during the study	42
Figure 6.8: Good sample observation of the image for AOI	44
Figure 6.9: Images locating presence of milling marks on the radio surface	44
Figure 6.10: Defining measurement points using the camera tool for radius check	45

List of Tables

Table 4. 1: Technical specification of UR 10 Robot derived from [27]	22
Table 4. 2: Technical specification of SICK PIM60 Inspector derived from [28]	22
Table 4. 3: Technical specification of the micro laser sensor derived from [29]	24
Table 4. 4: Technical specification of GRACO Dynamite Extruder derived from [31]	25
Table 5. 1: Technical specification of Cognex In-Sight 7905 camera derived from [32]	31
Table 5. 2: Various resolution and FOV of Cognex derived from [32]	35

1.Introduction

High competition and higher end expectation for efficiency, automating engineering operations has become the modern norm. In this master thesis work one such manually conducted engineering operation has been studied, investigated and attempted to automate [1].

The automation of complex industrial processes is an important topic in current robotics research. Especially in developing countries, a large effort is put into automation to keep the production in the countries rather than outsourcing to low-cost countries. Challenges arise when tasks that are complex are to be automated and the robot system must interact with an unknown environment or must handle unpredictable behavior of the work elements [2]. When controlling a robotic system, different control layers can be defined. The control problem is typically decomposed into three tasks: path planning, trajectory generation and trajectory tracking. Path planning deals with finding a collision free path that connects an initial configuration with a final configuration of the robot. Trajectory generation computes a time dependent function of the desired path which specifies the motion of the robot. The trajectory tracking is the task to control the robot to move on the desired trajectory [3].

The broad category of robots performing arbitrary tasks can be divided into four main areas. They are human-machine interaction, perception, intelligence and control. Feedback or Closed loop information is essential for communication and in identifying the requirements of a task to the robot and relate the progress. Perception plays a pivotal role for autonomous behavior and subjugates both lower end sensing and high-level abstraction of useful information about the world. The approaches implemented are dependent on the tasks [4]. Complex tasks require set of different approaches involve maintenance of consistent models, interpretation of high-level trajectory planning and conditioning and monitoring of actions. These activities are the functions of intelligence which serve as the link between control, interaction and perception. Robots undergo sophisticated challenges when trying to implement industrial applications. The interaction is expected to be robust and intuitive to perplexing interpretations [5]. Task objectives are more likely to be extemporary and hence not all applicable information is available. The desired behavior must be either inferred by the robot or actively pursued by prompting for further interaction. The robot might require learning new behaviors and shape their existing behavior based on the feedback. Sensor information is vital since sensing must provide measurements over variety of complex operating conditions. The robot must be capable of identifying and locating broad classes of objects in cluttered surroundings. Robot limb control must be robust to wear and other mechanical parameter variations. All such challenges should be encountered with real-time operation while the robot is to interact with humans naturally [6]. Although conveying all such challenges is beyond the scope of this thesis work, these challenges were considered while designing this robotic system. Visual perception has been introduced for robot control to provide feedback.

1.1 Motivation

The primary motivation for this thesis work is to bring more intelligence to the robot. To efficiently achieve this, this work has been sub-divided into two parts. In the first part of the work the manually conducted process task is automated with a visually enabled robot. The second part of the work involves introduction of a learning algorithm which isolates the active vision of the robot after the referencing. The main idea in automating the task was inspired from the organization's interest towards smart manufacturing ideologies [7]. Additionally, automating such task gradually contribute to the increase in accuracy and efficiency. It is also expected that this process automation might contribute to the profit by increasing the rate of output, however, the results are yet to be explored [8]. The latter part of this work is inspired by the modern-day boom in artificial intelligence. A learning algorithm which enables robotic control accounting positional deviations and misalignments isolating the vision system. However, the implementation of such learning algorithm is not covered in this thesis work as it is in its preliminary phase and organization's confidentiality concerns.

1.2 Task Objective

In this thesis work, a process task has been automated with UR 10 robot enabled with visual guidance. The process task to be automated is of dispensing operation. Here, dispensing of the thermal putty on the radio surface is the process that is being studied. Figure 1 shows thermal putty/gel dispensed radio surface. For the robot to maneuver dispensing on the surface of the robot, SICK PIM60 camera has been used as visual component. The camera enables the robot system to function under closed loop by providing visual feedback. In contrast with the current manual dispensing method, automating the task with the aid of robot manipulator would increase the efficiency of this operation. This is one of the main objectives of this automation. Primarily, the 2D camera and a laser sensor are used to identify the position of the radio surface (target object). The camera identifies the x and y coordinate while the laser sensor extracts the depth data or the z coordinate. After the identification of the reference points, the dispensing fiducial points are taught on a golden sample. The points are identified with eye level markings. As when the high-pressure nozzle arrives at these fiducial points the pneumatic valve is triggered which in turn delivers the thermal putty on the radio surface.

In parallel to this implementation various lighting conditions have been studied. The objective of studying various lighting conditions was to identify the most suitable condition to verify the volumetric analysis of the dispensed putty on the radio surface. After the justification of the imaging part, a mathematical model has been developed to comprehend the fiducial points of the target. The model has been mathematically simplified for the robot to perceive the coordinates. The simplified model is drawn into a script file which is stored in the robot's database. The fiducial point data obtained through the camera are streamed to this script file, where each fiducial point is identified as P_0 , P_1 , P_2 and P_3 . The controller has been designed with the help of prevailing Universal Robot's controller. Further extension of this task involves an implementation of a learning algorithm, which is not covered in this thesis work. The implication of using this learning algorithm is to isolate the application of visual component during the occurrences of disturbances causing offsets. In other words, when a radio arrives at the robot's envelope for dispensing

operation, the camera identifies the fiducial points, the dispensing takes place. While, the radio when it is on the conveyor, it can undergo some play which can cause deviation from the original path defining. Hence, this learning algorithm identifies the amount of deviation caused with the help of proximity sensors installed on the conveyor and accounts the offsets in the coordinates.

1.3 Literature Review and Background

Many researches have been carried out in the field of automation and robot control with vision guidance systems. Operation Management concepts have been accounted in a paper amidst collaborative robots in a manufacturing line [1]. This paper discusses the implications and the benefits involved in introducing these concepts in the manufacturing environment. It is very essential to study the Human-robot interaction in the industry. Such important attributes have been accounted in Jordi Viver Escalé's work [2]. The mechanics and dynamics on the Control of a Robotic Arm has been studied from M.R. de Gier. This research work further extends to provide insights in designing robotic systems with eye-in-hand camera configuration [3]. Since the thesis work involves pattern identification, investigation report written on Motion planning strategy was considered to study the implementation fundamentals of pattern recognition. There exist various methods for pattern recognition [4]. Fundamentally a marker is put on the object to be detected. These markers are usually patterning to be detected. Another alternate solution is cross correlation which is based on template matching [5]. This work also describes the Advances in 3D estimation and pose estimation in Robotic Applications. The usage of a laser sensor to extract depth data was studied and experimented independently. The motion planning strategy for the 6-DoF robot has been studied by Sven & Behnke [6] which explicitly briefs the conditions and parameters involved in robot trajectory planning.

Jessica Garcia Castano provides practical guidelines in implementing collaborative robots in an assembly line. This work highlights the key elements of the 4.0 Industry and Lean Manufacturing concepts [7]. Some insightful derivations were learnt to analyses the data extracted from the laser sensor. This study briefly explains sensor based real time control of industrial robots. Although the end effector for this process task has been outsourced and developed externally, the work by Burak Dogan on development of a two-fingered and a four-fingered robotic gripper has been considered to facilitate to design the end effector in-house. Due to reliable industrial finish the design and fabrication of the end effector took place externally [8].

Joni Sipponen pointed out the concerns while employing machine vision to a manufacturing line. This work covers in detail the implications involved in handling various lighting techniques. Some insights and conclusions for this thesis work have been drawn from this study as it involves experimentation with various machine vision lighting techniques [9]. Finally, Swagat Kumar et al. worked on design and development of an automated Robotic pick and stow system, which summarizes careful engineering approaches to be considered while automating a process task [10].

1.3.1 Justification for choosing current implementation.

Although many researches work related to pick and place and development of automation assembly lines were referred for this thesis work, Performance measurement of mobile manipulators by Roger B. provided preferable insights for this automation implementation task [11]. In this work the applications and advantages of using a 2D camera for measurement related tasks have been well explored and reported. The work also portrays the use of stereo vision camera and the difficulties in extracting datum. Computer vision for autonomous mobile robotic applications describe the methods for implementing pattern recognition methods for image processing [12]. Part detection for 3D models have been described and analyzed to give investigative details [13]. Automatic Optical Inspection methods were studied, and the inspection methods were convinced for an automotive assembly line. Based on this investigation, it provides justification that the proposed implementation method.

1.4 Thesis Structure

This thesis is organized in the following way. Chapter 2 is named as Conceptual Design, under which the existing manual operation method and the proposal for automation line is described. Under Chapter 3, a mathematical model has been developed. The importance of mathematical model is to identify the positional changes that occur due to deviations on the radio platform resulting in offsets in the defined fiducial points. Chapter 4 named as Implementation, outlines the entire implantation work carried out in this thesis work. Robot and camera setup, interfacing the camera and the laser sensor, setting up the GRACO extruder and pneumatic valve are some of the modules described under this chapter. At last, the chapter provides an overview of the implemented system. Chapter 5 describes the theory and experimental results of implementing various lighting techniques. This Chapter further elaborates the results from imaging with different setups if lighting conditions and pixel resolution calculation. Finally, this chapter proposes a solution for the hardware to be implemented. Chapter 6 provides insights and results from the study that was carried out to verify the volumes of thermal putty that are being dispensed on the surface of the radio surface. This feasibility study provides details on the experimental approaches and results from this study. Under Chapter 7 extensively outline the results of the machine vision study, feasibility study results and verification results from implementing this system in the manufacturing line. In Chapter 8 overall discussion on the implementation has been discussed. Chapter 9 summarizes the entire thesis work providing less detailed information on the future work.

2. Conceptual Design

High end electronics require the use of thermal interface materials due to efficient dissipation of temperature from its surface. These thermal materials accommodate through variety of gaps and form complex geometrics. This ability of thermally conductive, dispensable materials provides reduced thermal contact resistances and reduces the temperature on the surface and increase the efficiency of the electronic applications [8]. While considering dispensable products parameters such as pump equipment, mating surfaces, closure force and physical application of the material must be carefully thought of. There exist options for dispensing equipment ranging from manual syringes to high end high volume automated dispensing systems. The selection of such proper apparatus will depend upon factors such as volume, labor and equipment cost and material type to be dispensed. While considering suitable dispensing equipment, it is also important to pre-analyze how the equipment may interact with the material. The compatibility between the material and the dispensing system need to be studied to optimize equipment life and maintain material properties [9]. For higher thermal conductivity these materials are filled with ceramic particles. This causes the thermal compounds to have high viscosity and abrasiveness. Hence, the dispensing such thermal compounds will be different than low viscosity grease and adhesives. Once the proper equipment is selected, some factors need to be considered to increase the quality and throughput of the material. These factors include, nozzle height, dispensing pattern, dispensing speed, needle diameter etc. [10]. Similarly, in ERICSSON radios such thermal interface materials are being used to maintain equanimous temperature conditions. Thus far the process was carried out manually. The thermal putty is dispensed on the radio surface by an operator with the help of Nordson EFD 2K manual dispenser guns. It was observed with usage of manual dispensers the precise quantity of thermal putty expected on the radio surface is not met. Hence, this leads to poor thermal conductivity and wastage of putty material. The excess thermal material is not recycled. This is due to amalgamation of the putty with impurities.

2.1 Existing process method

The dispensing of thermal putty on the surface is carried out after the casted metal radio body has been fitted to the chassis. The casted metal radio body is where the thermal putty is being dispensed. The radio consists of power amplifiers which at times function at higher power causing high residual temperatures. Figure 2.1 shows the manually dispensed radio surface after a PCB board is being mounted. There exist methods to perform object recognition easily and successfully, for example, put a sticker with designed dot pattern.

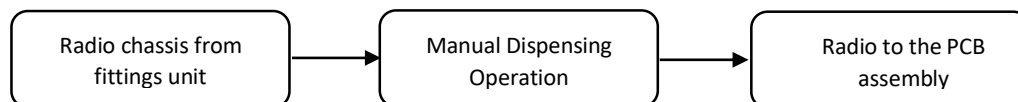


Figure 2.1: Existing Process task in manual mode

But it is less intelligent and inconvenient towards real practice. Taking one example in assistive robotics, each item to be grasped needs one sticker and add or change items require new sticker or change sticker.

In addition, sticker is easily being broken. It is convenient for research purpose but not suitable for practical application. Some machine learning-based methods are more intelligent and don't require a lot of maintenance as the previous one. But it requires a lot of training samples. The design unit recommends and decides the putty quantity to be dispensed on the surface. While working under manual condition, trained operators are given layout on where and how much putty to be dispensed. This layout presents the overview on exact amount of thermal material to be dispensed.

Figure 2.2 depicts one such layout that was presented by the design unit for putty quantities. In manual mode more considerations are only given to the start and end of putty pattern. Under normal condition, the putty pattern is a straight line. The design provides tolerance for the putty amounts. How the tolerance amount is decided is unknown. However, due to the tolerance limits, this helps in easing the operation.

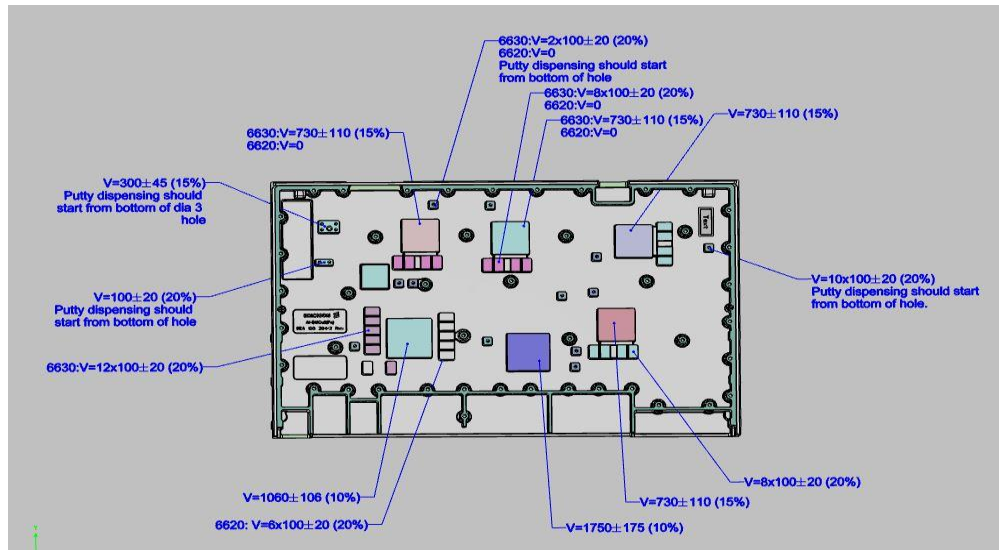


Figure 2.2: Thermal putty dispensing points recommended by Designers

The manual operation method comes with various challenges. One of the major challenges is the wrong amount of putty being dispensed. The wrong amount could be in excess or in scarce. The excess amount of putty material lead to material wastage while lesser amount lead to low thermal conductivity. A syringe valve (Figure 2.3) from Nordson was found ideal to be used for small-volume operations. This provides support to small quantity of material to be dispensed during production. Additionally, these dispensers are easy to set-up and its flexibility makes it preferable for future process developments. It has high chemical resistance. The changeovers are relatively simple due to the use of syringe.



Figure 2.3: Nordson manual dispensing gun derived from [30]

Changeovers are simple because the syringe is installed, as supplied from the fluid manufacturer, directly into the DV-01. It is not necessary to clean the DV-01. When the syringe is empty, or production is completed, the syringe is removed and the DV-01 is ready for use once more. Because there are no moving or wearable parts to be maintained, the cost-of-ownership is reduced to the consumable needle tip. The DV-01 is compatible with standard Nordson syringes, lure needle tips, and other brands that feature the same syringe dimensions and threads. Fluid flow is controlled by applying pressure to the syringe during 'valve on' and removing pressure from the syringe during 'valve off.'

2.2 Alternate method Proposal

As an alternate approach, it was proposed to automate the task with a vision guided robot system. In this alternate method manual dispenser gun is replaced by a high-pressure nozzle which is controlled pneumatically [11]. Although the system has its own complexities in automation, it was estimated, however, that this alternate approach would overcome or eliminate some of the challenges faced in the manual operation method. To implement this, change a 6-DoF robotic manipulator is required. As per company advise this Robot was decided to be Universal Robot's UR 10e. To extract the coordinate information a visual component is required. SICK PIM60 inspector was readily available in-house. Therefore, this 2D camera has been used for this implementation. With the help of a 2D camera only the positional information can be extracted. In other words, when the camera captures the image only the X and Y coordinate information is available. It is also important to extract the Z coordinate data. During the manual dispensing method, due to human interaction, the position of the target object is seldom considered to be an important parameter. Any misalignment can be easily accounted and supported by the operator. However, this is not a feasible option for a robot system. We have tolerance of 3mm for the dispensing needle to be above the target object. To achieve this a mathematical model was developed. This model describes the deviations that can be caused by any change on the product. The dimensional changes on the radio surface (target object) occur due to casting limits. Figure 2.4 portrays the proposed alternate method.

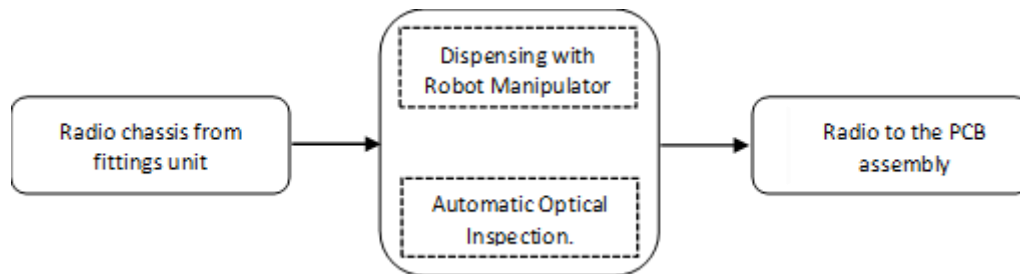


Figure 2.4: Proposed alternate dispensing method with robotic manipulator.

The changes that are caused in the Z coordinate, herein the height of the target object is measured with the aid of a micro laser sensor. The positional information, X, Y and Z coordinate information fed into a script file through robot manipulator's positions. The thermal material is dispensed through a high-pressure dispensing valve. The pressure valve is dispensed with the help of a valve regulator. Initially the camera references the corners on the radio surface. For computational convenience these corners are marked as P1, P2 and P3. All this information is recorded in a excel file. In this excel file the amount of thermal material to be dispensed is also defined. In addition to this, it is necessary to measure the quantity of the thermal material that is being dispensed on the radio surface.

3. Mathematical Modelling

This chapter briefly discusses the need for a mathematical model. Essentially, the casted product has tolerances present on its surface. Due to this conventional teaching of the robot to dispense the thermal putty on the radio surface is ineffective. In a conventional teaching method, offsets caused by tolerances are not accounted hence the system is subjected to fail under this condition. To effectively handle such situations a mathematical model has been developed [12]. Most geometric models in robotic vision systems involve transformations within and between three-dimensional Euclidean space R^3 and the two-dimensional space R^2 of the image plane. To distinguish these spaces, we adopt the convention of labelling vectors in R^3 using upper-case bold symbols such as X and vectors in R^2 using lower-case bold, as in X [13]. Analytical models can be cumbersome in Euclidean space since rotations, translations and camera projections are described by different linear and non-linear transformations. Under the alternative framework of projective geometry, all coordinate transformations are unified as linear matrix multiplications, known as homogeneous or projective transformations. Projective geometry is therefore used extensively in place of Euclidean geometry to model robotic and computer vision systems [14].

3.1 Vector Solution

In robotics, conventionally analytic reasoning is used, as cartesian coordinates are used to define robot tasks in cartesian workspace. It is essential to define a coordinate frame to assign the coordinates. We could specify the coordinates of the point P with respect to either frame XYZ or frame KLM. In the former case, we might assign to P the coordinate vector $(x_0, y_0, z_0)^T$ and in the latter case $(k_0, l_0, m_0)^T$. A notation is adopted such that the superscript used denotes the reference frame thus the reference frame is always clear. Figure 3.1 shows the mathematical model used to develop the vector solution.

In the above schematic diagram, X, Y, Z represent the coordinate axes of the robot, and K, L, M represent the coordinate axes of the object (the radio surface). O being the origin of the system.

The coordinate shift vector is represented by \vec{N} The vector start points O is defined at the coordinate points (0, 0, 0) and the vector endpoint PO is defined at the coordinate points (x_0, y_0, z_0) . This means the resultant coordinate axis shift vector can be obtained by subtracting the vector end points and the vector start points. It is understandable that the resultant coordinate will be represented x_0, y_0, z_0 coordinate frame. The resultant equation is represented as equation 3.1.

$$\vec{N} = PO (x_0; y_0; z_0) - O(0; 0; 0) = \vec{N} (x_0 - 0; y_0 - 0; z_0 - 0) = \vec{N} (x_0; y_0; z_0) \quad (3.1)$$

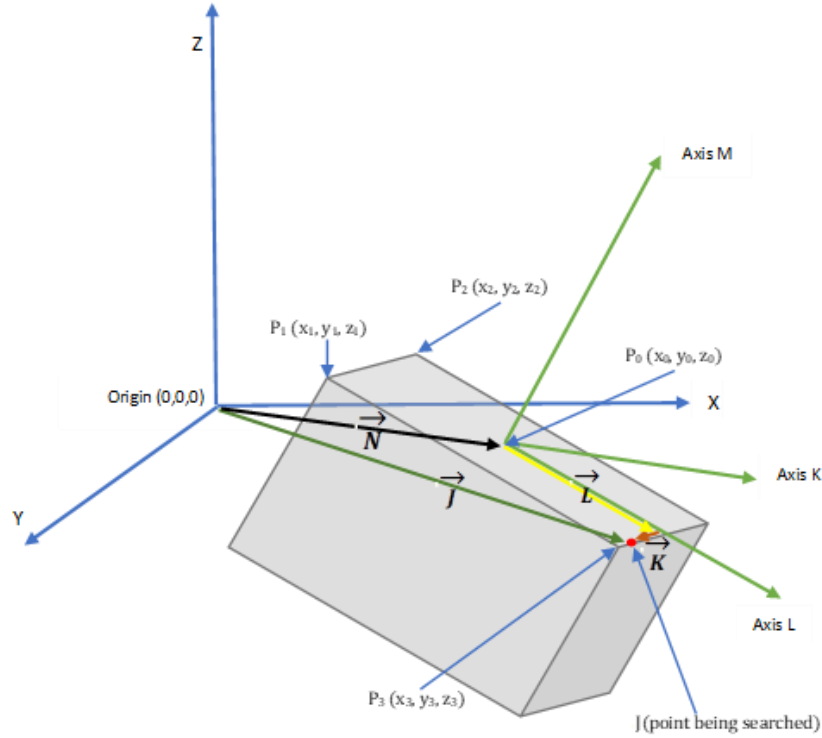


Figure 3.1: Mathematical Model denoted with various coordinate systems

It is important to account vectors \vec{J} , \vec{L} and \vec{K} to locate the point that is being searched on the radio surface, here the point being searched is denoted by J. Vector \vec{K} lies in the same direction as in the vectors joining the points P1 and P2. It can be inferred that the length of this vector is the value of the resultant k-coordinate on point J as the vector lies on k-coordinate axis.

Equation 3.2 describes the coordinates of the K-coordinate axis direction vector system.

$$\overline{P1P2} = P2 (x_2; y_2; z_2) - P1 (x_1; y_1; z_1) = \overline{P1P2} (x_2 - x_1; y_2 - y_1; z_2 - z_1) \quad (3.2)$$

Equation 3.3 describes the length of the direction vector on the K-coordinate system,

$$|\overline{P1P2}| = \sqrt{(x_2 - x_1)^2 + (y_2 - y_1)^2 + (z_2 - z_1)^2} \quad (3.3)$$

In conclusion, to obtain \vec{K} , which is parallel to points P1, P2 and length k, the vector $|\overline{P1P2}|$ coordinates with the length ratios. Equation 3.4 describes the resultant vector \vec{K} .

$$\vec{K} \left(\frac{x_2 - x_1}{\sqrt{(x_2 - x_1)^2 + (y_2 - y_1)^2 + (z_2 - z_1)^2}}; \frac{y_2 - y_1}{\sqrt{(x_2 - x_1)^2 + (y_2 - y_1)^2 + (z_2 - z_1)^2}}; \frac{z_2 - z_1}{\sqrt{(x_2 - x_1)^2 + (y_2 - y_1)^2 + (z_2 - z_1)^2}} \right)$$

$$\vec{K} \left(\frac{k(x_2 - x_1)}{\sqrt{(x_2 - x_1)^2 + (y_2 - y_1)^2 + (z_2 - z_1)^2}}; \frac{k(y_2 - y_1)}{\sqrt{(x_2 - x_1)^2 + (y_2 - y_1)^2 + (z_2 - z_1)^2}}; \frac{k(z_2 - z_1)}{\sqrt{(x_2 - x_1)^2 + (y_2 - y_1)^2 + (z_2 - z_1)^2}} \right) \quad (3.4)$$

Similarly, to find \vec{L} , it lies on the same direction as in the vector joining the points P1 and P3, and the length of this vector is the value of L-coordinate of the point J. Equation 3.5 describes the length vector on the L-coordinate of the point J.

$$\vec{L} \left(\frac{l(x_3 - x_1)}{\sqrt{(x_3 - x_1)^2 + (y_3 - y_1)^2 + (z_3 - z_1)^2}}; \frac{l(y_3 - y_1)}{\sqrt{(x_3 - x_1)^2 + (y_3 - y_1)^2 + (z_3 - z_1)^2}}; \frac{l(z_3 - z_1)}{\sqrt{(x_3 - x_1)^2 + (y_3 - y_1)^2 + (z_3 - z_1)^2}} \right) \quad (3.5)$$

It is necessary to consider the components in the direction of the coordinate axis M-coordinate axis of the detail. M is perpendicular to vectors P1P3 and P1P2 (not shown on the graph). The vector M whose direction vector M (length does not match M-coordinate, but the direction corresponds), we find P1P3 and P1P2.

$$\vec{M}_s(x_{ms}; y_{ms}; z_{ms}) = \vec{P1P3} \times \vec{P1P2} = \begin{vmatrix} x_{ms} & y_{ms} & z_{ms} \\ x_3 - x_1 & y_3 - y_1 & z_3 - z_1 \\ x_2 - x_1 & y_2 - y_1 & z_2 - z_1 \end{vmatrix}$$

$$x_{ms} = (y_3 - y_1)(z_2 - z_1) - (z_3 - z_1)(y_2 - y_1)$$

$$y_{ms} = (z_3 - z_1)(x_2 - x_1) - (x_3 - x_1)(z_2 - z_1)$$

$$z_{ms} = (x_3 - x_1)(y_2 - y_1) - (y_3 - y_1)(x_2 - x_1) \quad (3.6)$$

Equation 3.7 describes the length of the \vec{M} as seen below.

$$|\vec{M}_s| = \sqrt{x_{ms}^2 + y_{ms}^2 + z_{ms}^2}$$

$$|\vec{M}_s| = \sqrt{\{(y_3 - y_1)(z_2 - z_1) - (z_3 - z_1)(y_2 - y_1)\}^2 + \{(z_3 - z_1)(x_2 - x_1) - (x_3 - x_1)(z_2 - z_1)\}^2 + \{(x_3 - x_1)(y_2 - y_1) - (y_3 - y_1)(x_2 - x_1)\}^2} \quad (3.7)$$

To quantify the \vec{M} , which is parallel to the \vec{M}_s and the length M, the entire equation is divided with the length ratios.

$$\vec{M} \left(\frac{m\{(y_3 - y_1)(z_2 - z_1) - (z_3 - z_1)(y_2 - y_1)\}}{\sqrt{\{(y_3 - y_1)(z_2 - z_1) - (z_3 - z_1)(y_2 - y_1)\}^2 + \{(z_3 - z_1)(x_2 - x_1) - (x_3 - x_1)(z_2 - z_1)\}^2 + \{(x_3 - x_1)(y_2 - y_1) - (y_3 - y_1)(x_2 - x_1)\}^2}}; \right. \\ \left. \frac{m\{(z_3 - z_1)(x_2 - x_1) - (x_3 - x_1)(z_2 - z_1)\}}{\sqrt{\{(y_3 - y_1)(z_2 - z_1) - (z_3 - z_1)(y_2 - y_1)\}^2 + \{(z_3 - z_1)(x_2 - x_1) - (x_3 - x_1)(z_2 - z_1)\}^2 + \{(x_3 - x_1)(y_2 - y_1) - (y_3 - y_1)(x_2 - x_1)\}^2}}; \right. \\ \left. \frac{m\{(x_3 - x_1)(y_2 - y_1) - (y_3 - y_1)(x_2 - x_1)\}}{\sqrt{\{(y_3 - y_1)(z_2 - z_1) - (z_3 - z_1)(y_2 - y_1)\}^2 + \{(z_3 - z_1)(x_2 - x_1) - (x_3 - x_1)(z_2 - z_1)\}^2 + \{(x_3 - x_1)(y_2 - y_1) - (y_3 - y_1)(x_2 - x_1)\}^2}} \right) \quad (3.8)$$

It is important to get the resultant vector to determine the resultant coordinates for the robot manipulation. The resultant vector \vec{J} is obtained by summing up \vec{N} , \vec{J} , \vec{L} and \vec{K} . Equation 3.9 describes the resultant and the system coordinates of \vec{J} .

$$\vec{J} = \vec{N} + \vec{K} + \vec{L} + \vec{M}$$

$$\vec{J} \left(x_0 + \frac{k(x_2 - x_1)}{\sqrt{(x_2 - x_1)^2 + (y_2 - y_1)^2 + (z_2 - z_1)^2}} + \frac{l(x_3 - x_1)}{\sqrt{(x_3 - x_1)^2 + (y_3 - y_1)^2 + (z_3 - z_1)^2}} \right. \\ \left. + \frac{m\{(y_3 - y_1)(z_2 - z_1) - (z_3 - z_1)(y_2 - y_1)\}}{\sqrt{\{(y_3 - y_1)(z_2 - z_1) - (z_3 - z_1)(y_2 - y_1)\}^2 + \{(z_3 - z_1)(x_2 - x_1) - (x_3 - x_1)(z_2 - z_1)\}^2 + \{(x_3 - x_1)(y_2 - y_1) - (y_3 - y_1)(x_2 - x_1)\}^2}}; y_0 \right. \\ \left. + \frac{k(y_2 - y_1)}{\sqrt{(x_2 - x_1)^2 + (y_2 - y_1)^2 + (z_2 - z_1)^2}} + \frac{l(y_3 - y_1)}{\sqrt{(x_3 - x_1)^2 + (y_3 - y_1)^2 + (z_3 - z_1)^2}} \right. \\ \left. + \frac{m\{(z_3 - z_1)(x_2 - x_1) - (x_3 - x_1)(z_2 - z_1)\}}{\sqrt{\{(y_3 - y_1)(z_2 - z_1) - (z_3 - z_1)(y_2 - y_1)\}^2 + \{(z_3 - z_1)(x_2 - x_1) - (x_3 - x_1)(z_2 - z_1)\}^2 + \{(x_3 - x_1)(y_2 - y_1) - (y_3 - y_1)(x_2 - x_1)\}^2}}; z_0 \right. \\ \left. + \frac{k(z_2 - z_1)}{\sqrt{(x_2 - x_1)^2 + (y_2 - y_1)^2 + (z_2 - z_1)^2}} + \frac{l(z_3 - z_1)}{\sqrt{(x_3 - x_1)^2 + (y_3 - y_1)^2 + (z_3 - z_1)^2}} \right. \\ \left. + \frac{m\{(x_3 - x_1)(y_2 - y_1) - (y_3 - y_1)(x_2 - x_1)\}}{\sqrt{\{(y_3 - y_1)(z_2 - z_1) - (z_3 - z_1)(y_2 - y_1)\}^2 + \{(z_3 - z_1)(x_2 - x_1) - (x_3 - x_1)(z_2 - z_1)\}^2 + \{(x_3 - x_1)(y_2 - y_1) - (y_3 - y_1)(x_2 - x_1)\}^2}} \right) \quad (3.9)$$

From the system coordinates obtained for \vec{J} from equation 3.9, the vector endpoint coordinates of the vector associated with the vector's origin. The origin of \vec{J} is zero (0, 0, 0) of the system coordinates and the end points are \vec{J} (x_j, y_j, z_j). The coordinates of the vector's origins are zeros and the coordinates of the point \vec{J} are the coordinates of the vector. Equation 3.10, 3.11 and 3.12 describe the results of x_j, y_j and z_j coordinates.

$$x_j = x_0 + \frac{k(x_2 - x_1)}{\sqrt{(x_2 - x_1)^2 + (y_2 - y_1)^2 + (z_2 - z_1)^2}} + \frac{l(x_3 - x_1)}{\sqrt{(x_3 - x_1)^2 + (y_3 - y_1)^2 + (z_3 - z_1)^2}} + \\ \frac{m\{(y_3 - y_1)(z_2 - z_1) - (z_3 - z_1)(y_2 - y_1)\}}{\sqrt{\{(y_3 - y_1)(z_2 - z_1) - (z_3 - z_1)(y_2 - y_1)\}^2 + \{(z_3 - z_1)(x_2 - x_1) - (x_3 - x_1)(z_2 - z_1)\}^2 + \{(x_3 - x_1)(y_2 - y_1) - (y_3 - y_1)(x_2 - x_1)\}^2}} \quad (3.10)$$

$$y_j = y_0 + \frac{k(y_2 - y_1)}{\sqrt{(x_2 - x_1)^2 + (y_2 - y_1)^2 + (z_2 - z_1)^2}} + \frac{l(y_3 - y_1)}{\sqrt{(x_3 - x_1)^2 + (y_3 - y_1)^2 + (z_3 - z_1)^2}} + \\ \frac{m\{(z_3 - z_1)(x_2 - x_1) - (x_3 - x_1)(z_2 - z_1)\}}{\sqrt{\{(y_3 - y_1)(z_2 - z_1) - (z_3 - z_1)(y_2 - y_1)\}^2 + \{(z_3 - z_1)(x_2 - x_1) - (x_3 - x_1)(z_2 - z_1)\}^2 + \{(x_3 - x_1)(y_2 - y_1) - (y_3 - y_1)(x_2 - x_1)\}^2}} \quad (3.11)$$

$$z_j = z_0 + \frac{k(z_2 - z_1)}{\sqrt{(x_2 - x_1)^2 + (y_2 - y_1)^2 + (z_2 - z_1)^2}} + \frac{l(z_3 - z_1)}{\sqrt{(x_3 - x_1)^2 + (y_3 - y_1)^2 + (z_3 - z_1)^2}} + \\ \frac{m\{(x_3 - x_1)(y_2 - y_1) - (y_3 - y_1)(x_2 - x_1)\}}{\sqrt{\{(y_3 - y_1)(z_2 - z_1) - (z_3 - z_1)(y_2 - y_1)\}^2 + \{(z_3 - z_1)(x_2 - x_1) - (x_3 - x_1)(z_2 - z_1)\}^2 + \{(x_3 - x_1)(y_2 - y_1) - (y_3 - y_1)(x_2 - x_1)\}^2}} \quad (3.12)$$

To convenient robotic manipulation Equations 3.10, 3.11 and 3.12 have been simplified and described in 3.13, 3.14 and 3.14.

$$x_j = x_0 + \frac{k \times X21}{P1P2} + \frac{l \times X31}{P1P3} + \frac{m \times XMS}{MS} \quad (3.13)$$

$$y_j = y_0 + \frac{k \times Y21}{P1P2} + \frac{l \times Y31}{P1P3} + \frac{m \times YMS}{MS} \quad (3.14)$$

$$z_j = z_0 + \frac{k \times Z21}{P1P2} + \frac{l \times Z31}{P1P3} + \frac{m \times ZMS}{MS} \quad (3.15)$$

Equations 3.16 through 3.27 describe the simplified coordinate calculations for robotic manipulation.

$$P1P2 = \sqrt{X21^2 + Y21^2 + Z21^2} \quad (3.16)$$

$$P1P3 = \sqrt{X31^2 + Y31^2 + Z31^2} \quad (3.17)$$

$$MS = \sqrt{XMS^2 + YMS^2 + ZMS^2} \quad (3.18)$$

$$XMS = Y31 \times Z21 - Z31 \times Y21 \quad (3.19)$$

$$YMS = Z31 \times X21 - X31 \times Z21 \quad (3.20)$$

$$ZMS = X31 \times Y21 - Y31 \times X21 \quad (3.21)$$

$$X21 = (x_2 - x_1) \quad (3.22)$$

$$X31 = (x_3 - x_1) \quad (3.23)$$

$$Y21 = (y_2 - y_1) \quad (3.24)$$

$$Y31 = (y_3 - y_1) \quad (3.25)$$

$$Z21 = (z_2 - z_1) \quad (3.26)$$

$$Z31 = (z_3 - z_1) \quad (3.27)$$

4.Implementation

4.1 Hardware Setup

The 6-DoF manipulator used is UR10e, a collaborative robot developed by Universal-Robots. Table 4.1 is the data of UR10e [27].

Payload	10 kg
Reach	1300 mm
Joint Range	$\pm 360^\circ$
Repeatability	± 0.1 mm
Speed	Joint: 180° /s Tool: 1000 mm/s
Communication	TCP/IP 100 Mbit: IEEE 802.3u, 100BASE-TX Ethernet socket & Modbus TCP

Table 4. 1: Technical specification of UR 10 Robot derived from [27]

The SICK inspector PIM60 is used for dispensing thermal putty on the surface of the radio. So, in that purpose we are going to use SOPAS Engineering tool which is compatible with SICK inspector PIM60 camera and a robot UR10e to move according to camera inputs [28]. This mean that in real time we must configure our image and take offset data from camera to move the robot accordingly at offset coordinates. Table 4.2 displays some of specifications of PIM60 camera.

Sensor	CMOS matrix sensor
Focus	Manually adjustable focus
Lens	M12 mount
Optical format	1/3"
Dimensions	100 mm x 52 mm x 38 mm
Resolution	384 px x 384 px 640 px x 480 px

Table 4. 2: Technical specification of SICK PIM60 Inspector derived from [28]

As shown in Figure 4.1 we made a network using switch that connects to our PC in which we have SOPAS engineering + Robot Controller (In which we input offset data) + SICK inspector PIM60 camera (from which we take Inputs). In Chapter 3 equation 3.17 through 3.26 denote the equation that can be used to provide these offset values to the robot movement. The initial pattern is defined in the SOPAS engineering tool using polygon and geometrical shapes, the camera tries to move to identify the pattern. Under the case of not using these equations, and when the camera is unable to find the pattern on the target object the camera is unable to detect the image of the radio surface.

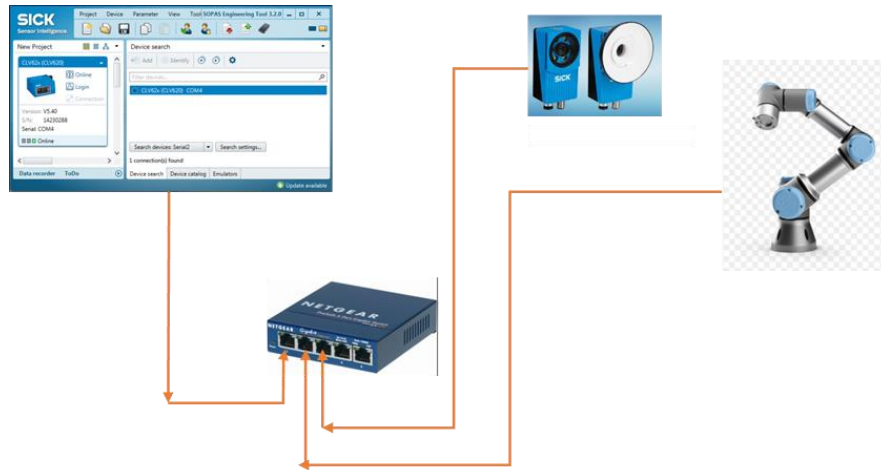


Figure 4.1: Overview of the communication setup for camera and robot

As shown in Figure 4.1 camera and the laser sensor are assembled together with the help of a holder. Appendix A provides information on the assembly drawings. The organization's interest in choosing PIM60 comes from the multi-functional vision toolbox which offers with performance and ease of use. The measurements taken from the camera are simple pass or fail verification over the exact measurement value. It is also important to note that the calibration ensures reliable inspection results. The results can be reliable even during the objects are being moved or being rotated and even under wide angle lenses the results are reliable. The resultant calibration data gives easily comprehensible mm data. The in-built webserver provides cost efficient analysis and monitoring. The ease of customizing an interface to suit the requirement is also one of the reasons to choose the camera workaround. Hence, this implementation does not require high-end programming. Further, to extract the Z coordinate data, Panasonic Micro distance sensor is being used [29]. This device offers help over mechanical measurement devices. The device was preferred due to its small measurement area, high-speed data collection and flexible operation. Laser sensors have the capability to attain high-speed measurements. Panasonic laser sensor provide repeatable measurements without the risk of moving the object. This laser sensor can also measure the vibration of a rotating components in real time. However, this feature is not applicable for our current implementation. The sensor has a robust housing to withstand heavy-duty industrial applications. With the help of this sensor, the distance to the product is taught. Figure 4.2 shows the Panasonic laser sensor that is being used in this implementation.



Figure 4.2: Panasonic ME-HGC1000 micro laser sensor derived from [29]

Since, the sensor does not involve mechanical probes, there is minimal risk of damage to the sensor and the sensor does not require frequent calibration. This feature reduces the costs. These sensors offer increased performances based on surface finishing of the component that is being projected at. Automatic laser power and measurement rate control ensures that the reliable measurements are unchanged under challenging target conditions. To meet the application requirements, the measurement rate can be fixed when a constant measurement rate is necessary. Table 4.3 outlines some of the important parameters of the Panasonic laser sensor [29].

Measurement Center Distance	50 mm
Measurement Range	± 15 mm
Repeatability	$\pm 360^\circ$
Linearity	$\pm 0.1\%$ F. S
Beam Diameter	Approx. $\varnothing 70\mu\text{m}$
Power Consumption	40mA or less

Table 4. 3: Technical specification of the micro laser sensor derived from [29]

After the camera and the laser sensor extract the position information and sent to the robot controller, based on this information the dispensing nozzle which is pneumatically controlled, dispenses the thermal material. Figure 4.3 illustrates the Nordson High pressure dispense valve system. 4 types of valves can be installed to the system. Valves can be connected and disconnected by tightening and loosening quick change system screw [30]. When air pressure at 4.8 bar is applied, the piston shifts the spool to open position which allows the fluid to flow. At the end of the cycle, spring force on the piston shifts the spool to the closed position. Valve assembly diagram is available in Appendix A. The valve system is controlled pneumatically. This means, when the robot controller provides digital signal, the valve system dispenses the thermal material.



Figure 4.3: Nordson 736HPA-NV pressure dispenses valve system derived from [30]

The Nordson high pressure valve system was selected for this implementation because, since the manual dispenser was available from the same supplier, it was convenient for future services. The stainless-steel high-pressure valve features adjustable stroke control to keep consistent dot profiles and bead widths and prevent drooling between shots. The chromium plated spool works with fluid inlet and outlet of ¼ NPT. The adjustable stroke control also helps in reducing the opening surge and regulates the cut-off. Some of the valuable features include, opening surge control, adjustable snuff-back cutoff, auxiliary air inlet air-assist closure and compact size and weight. Compatible fluids that can be used with these high-pressure valves are adhesives, greases and sealants. Table 4.4 outlines the technical specification Nordson High-Pressure valve system.

Size	134.4 mm length x 34.9 mm diameter
Actuating pressure	4.8 bar
Fluid inlet thread	¼ NPT female
Cycle rate	Exceeds 400 per minute
Spool	Stainless, hard chrome coated
Piston	Hard-coated aluminum

Table 4. 4: Technical specification of GRACO Dynamite Extruder derived from [31]

A pumping system is required to pump the thermal material. For this Dynamite Extruder has been used. This precision dispense system can pump single component viscous materials. Some of the features and benefits of this system include its nature of compact and lightweight, extrudes viscous materials from their original quantity, built-in tough and rugged conditions and ram includes 3” air cylinders to handle thick materials [31]. Typical applications these extruders are used at dispensing viscous fluids and pastes, manual and automatic valve applications and industrial workbench applications. These systems can handle fluids such as adhesives, thermal pastes, sealants, heatsink compounds etc. Figure 4.4 illustrates the Dynamite Extruder that is being used in this implementation.



Figure 4.4: GRACO Dynamite Extruder derived from [31]

4.2 Overview of the System

In this section the overview of the system will be outlined. Figure 4.8 illustrates how every independent system block are configured for this implementation. When a needle tip is different from the old one more than 2.5 mm from any axis you should reattach the TCP [17]. In other cases, you should reattach needles. When prompted with which needle to be taught, the valve number is pressed. Further, the robot will move the needle to the desired position. Figure 4.5 shows how the products are referenced with the help of SICK PIM60 camera.

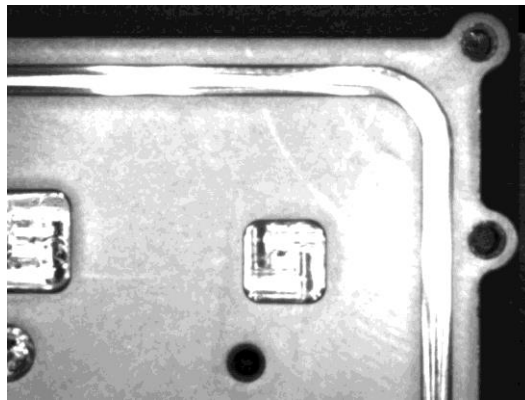


Figure 4.5: Image of the radio surface acquired from SICK PIM60 camera

On the image that is being captured by the camera, geometric images are drawn as shown below. When on run mode when the camera tries to fetch these defined patterns [18]. The mathematical model that was developed helps in identifying the coordinate system for the robot manipulator to maneuver to the desired position on the radio surface accounting the offsets. As mentioned earlier these offsets result from the tolerances and casting inaccuracies.

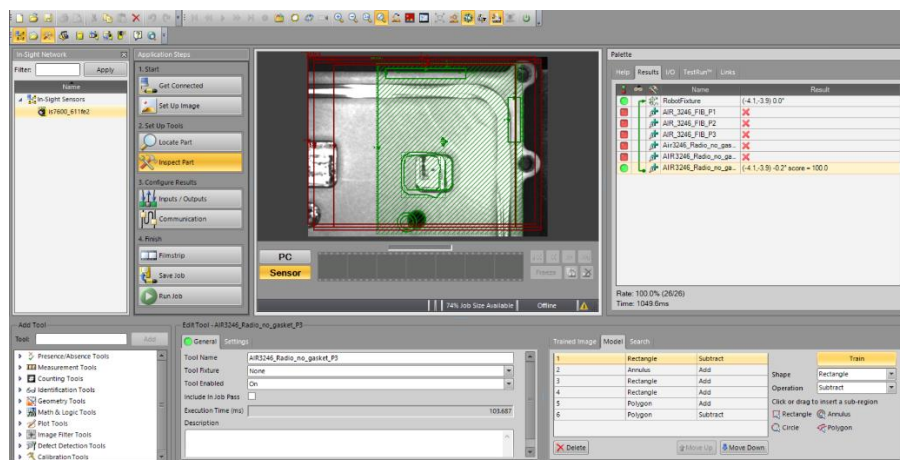


Figure 4.6: Introducing geometrical shapes on the obtained image with camera tool

From I/O Tab turn Laser Power is turned on. In the opened program there is 3 waypoints. These points use laser TCP. The laser is moved on top of the selected corner P1. While this action takes place, the output signal on the laser should be on. This can be tested by moving the robot higher up by 1 mm and it should be turned off. The TCP RZ should be 270 degrees or 4.712 radians [19]. Repeat the step in every chosen corner.

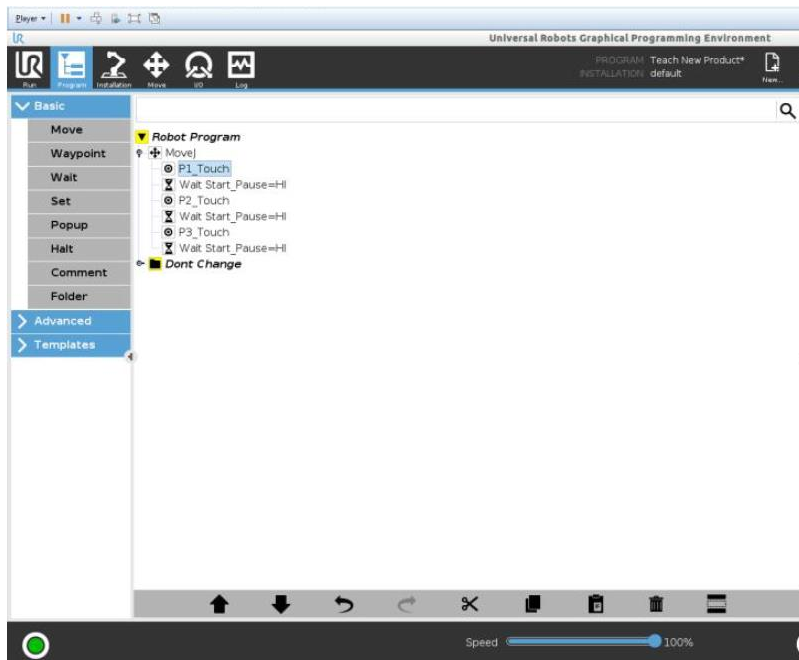


Figure 4.7: Initialization of the hardware from the robot controller

After the robot is started the robot will move to do the corners and waits in every corner for the green button to be pressed. This is verified visually to ensure the laser is in right position. After the green button is pressed on P3 the robot will move over the corners with the camera and waits at every corner for the green button press. The camera is connected using the SOPAS tool software and the setup of the dispensing positions in every corner first. The camera sends the coordinates using the robot tool fixture. The newly created locations on the surface use the X and Y coordinate outputs. These steps are repeated on every corner of the product. When the camera job is setup on P3 then the information is saved in Sick job file while the camera is in online mode [20]. The number of variables is inserted in the provided excel file. The points and amount of the thermal material is also defined in the excel file. After generating the script file as .script extension on a USB memory stick, in robot pendant the Main program is run. The else if statements are added to do the function with desired conditions.

The default installation file is opened to set the valve flow rate. The variables which are present as SET_V (valve number) are edited with the desired values. The units can be in millimeters or grams. These variables show how much thermal material will flow from the needle in one second. When the unit is changed, the script file also needs to be updated.

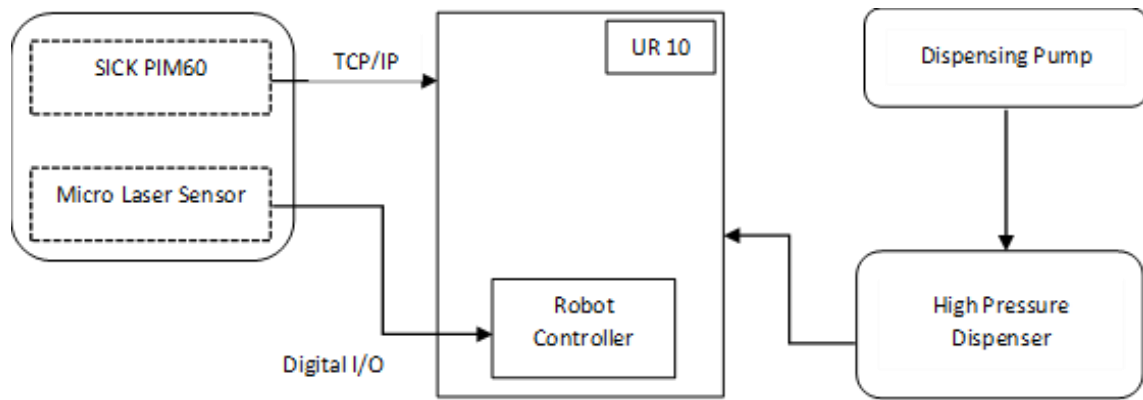


Figure 4.8: Overview of the system configuration

5. Inspection

The process should be controlled to achieve expected results. Proper maintenance and observation of factors which can affect the machine's ability to dispense correctly should be corrected regularly. If it is noticed that these factors are not correct or improper in any machine, then issue should be escalated to responsible person to solve the problem [21]. The process should be controlled to achieve expected results. Proper maintenance and observation of factors which can affect the machine's ability to dispense correctly should be corrected regularly. If it is noticed that these factors are not correct or improper in any machine, then issue should be escalated to responsible person to solve the problem. The pressure should be regulated and stable for machine as well as pail pump. Deviation in one of these pressure points, can cause irregularities in dispensing. In case of Graco, pump/motor pressure L should be 50 PSI, ram pressure R should be 40 PSI and fluid regulator valve pressure should be 20 PSI. In case of 6-axis robot, pump/motor pressure L should be 60 PSI, ram pressure R should be 50 PSI. All programs should be created according to these pressure values in each machine. Homing is necessary to calibrate the Graco machines after every small disturbance or long stops during dispensing process to avoid inaccuracy. The nozzle must be cleaned before homing otherwise the machine can be calibrated in a wrong way. It is necessary to purge some material after every small disturbance or long stops during dispensing process to avoid irregular/less putty flow. A small purging program should be created for both machines to run before starting of every shifts or long breaks [21] [22].

The nozzle should be clean and without any clogs to ensure smooth dispensing. Also, the nozzle must be cleaned before homing otherwise the machine can be calibrated in a wrong way. If the material is continuously dripping, then maintenance is required immediately. The nozzle should be ideally at 3.0 ± 0.3 mm height from the dispensing surface to get smooth dispensing pattern. Higher nozzle can result in spiral type patten and lower height can result in wide pressed pattern, while both can result in non-stickiness of putty to the surface. Under this chapter an important challenge in automating this process task has been investigated. The challenge being to study the volume of the dispensed putty. Yet, for this visual feedback system the most important factor is lighting. Since the lighting and various lighting techniques are involved in acquiring suitable image for further investigation.

Vision is an ideal modality for robots when introducing intelligence in their behavior. The feedback from vision sensors to the robot consists of rich information about the environment required for perception and understanding navigating conditions in real time. Additionally, vision-guided robots may not be calibrated frequently which is of great practical benefit. The vision capabilities simple binary image processing to sophisticated edge-based and feature-based system. In an open loop system, the visual sensing and manipulation are coupled for looking then moving condition. The efficiency of such systems highly related to the precision of the visual sensor and the robot manipulator. An alternate approach would be a to introduce a visual feedback control loop. The great advantage of feedback control is the accuracy of these systems can be less sensitive to calibration errors and non-linearities. The camera used could be stationary or used in robots' hand. The latter condition is referred to as eye-in-hand configuration. For the experiments conducted in this thesis work, stationary position of the camera in idealized. A visual system can perform functions such as, image acquisition and analysis, recognition of an

object. The process of image acquisition involves a photo detector is used to generate an optical image that can be generated in to digital image. The process further involves, image sensing, representation of image data and digitization.

A visual system can perform the following functions: the image acquisition and analysis, the recognition of an object or objects within an object group. As can be seen in Figure 5.1, the light from a source illuminates the scene and an optical image is generated by image sensors. Image acquisition is a process whereby a photo detector is used to generate an optical image that can be converted into a digital image [23]. This process involves the image sensing, representation of image data, and digitization. Image processing is a process to modify and prepare the pixel values of a digital image to produce a more suitable form for subsequent operations. The main operations performed in the image processing are outlined. Segmentation seeks to partition an image into meaningful regions that correspond to part or whole objects within the scene. Feature extraction in general seeks to identify the inherent characteristics, or features, of objects found within an object. Pattern classification refers to the process in which an unknown object within an image is identified as being part of one group among several possible object groups [24].

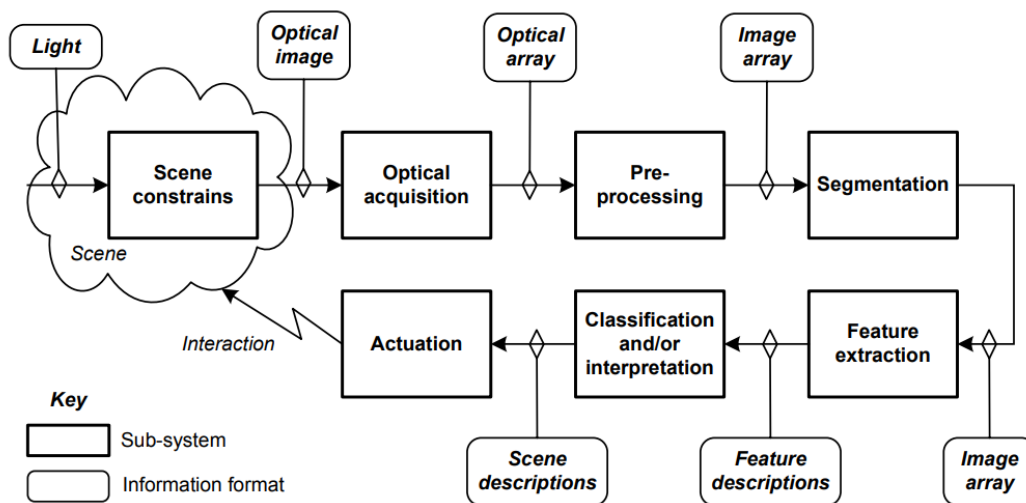


Figure 5.1: Block diagram of a typical vision system [5]

A standard machine vision system involves several components such as, digital or analogue cameras, camera interface to digitize image, processor (normally PC or embedded processor such as DSP), communication links, specialized light source, software for image detection of features etc. In any vision-based systems/applications the illumination plays a pivotal part for the system's efficiency. At a fundamental level there must be enough light for the camera to acquire a good image. Further, it is also necessary to consider orientation, geometry or color of the light to differentiate relevant information and to distort irrelevant parts of the image [24]. There exist three main types of light sources, filament bulbs which work by passing electric current through a metal filament, discharge lamps which uses an electric arc through an inert atmosphere to create light and light-emitting diodes which use semiconductor devices where electro-luminescence occur in p-n junction [25].

5.1 Problem Statement

Ericsson has devices that are dispensing thermal gel on die cast machined surfaces. There are quality issues on dispensing. As discussed in Chapter 2 under existing process method these quality issues can be roughly classified into two categories such as, incorrect amount is dispensed, and thermal material dispensed at an incorrect position or angle or both at times. The objective of this chapter is to experiment various lighting techniques and thereby to find out the most suitable lighting techniques to be used on the product. For experimentation in this thesis work Cognex In-Sight 7905 Smart Camera has been used. Although SICK PIM60 smart camera has been used as the visual component on the robot hand, Cognex smart camera has been used to capture the radio surface images under various lighting conditions.

Sensor	CMOS
Acquisition Rate	32 fps
Lens	C mount
Image Type	Monochrome
Image Processing Memory	512 MB
Internal Light Color	Red, White, IR or Blue
Power	24 VDC

Table 5. 1: Technical Specification of Cognex In-Sight 7905 camera derived from [32]

For this study only 2 Dimensional components are studied. This means that the amount (volume) of dispensed thermal material is not measured. Instead, the experimentation was conducted under the assumption that certain area of gel has certain shape and therefore, certain volume. Below Figure 5.2 illustrates the test setup with camera for various lighting conditions. The camera is stationary mounted. Two Infrared opposite facing light sources have been mounted.

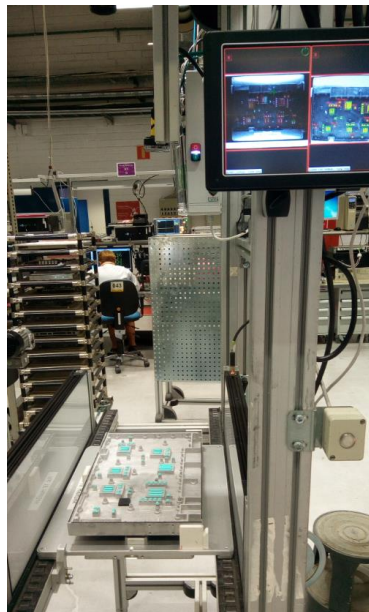


Figure 5.2: Test setup for Automatic Optical Inspection

5.2 Machine Vision Lighting

Vision Lighting is one of the most critical aspects of machine vision applications. Failing to suitably illuminate the object results in loss of information and efficient producibility [32]. A proper lighting technique involves a light source and its placement with respect to the part and the camera. Different forms and geometries of lighting were tested. Purpose was to find lighting geometry, that would give best contrast with all color combinations of mechanics and gels.

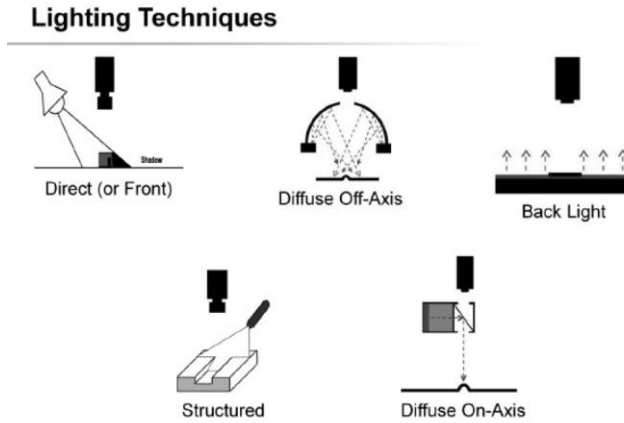


Figure 5.3: Illumination techniques used in Machine Vision derived from [32]

Back Lighting techniques provides illumination from behind the target highlighting the silhouette of the target. Figure 5.4 illustrates the test setup for Back Light technique. This lighting type is used to detect presence of thermal material and to measure its quantity by measuring the outline shape. Since contrast is an important element in here, with this technique the surface detail is lost. This type of lighting is most suited when the component is situated on a glass plate and transported in a guide rail. And it is also most suitable when the component is held by the robot gripper or a gripper system above the light.



Figure 5.4: Experimental setup for Back Light illumination technique

Diffuse dome lighting eliminates LED glares and shadows under illumination. This type of lighting is best suited for preventing halo effect. Ring lighting mostly finds its application in coating inspection and inspection of PCB. Ring lighting scatters the light, this prevents incoming glare from reflective parts. This technique can be recommended for all directional lighting for uniform spread of light across the target. The technique is handy in reducing lighting noise like glare and hotspots from directional lights such as ring lights. Figure 5.5 depicts the test setup for this illumination technique.

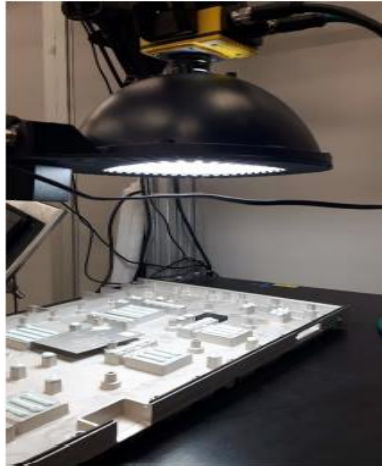


Figure 5.5: Experimental setup for diffused dome light illumination technique

The experimental setup for ring light is a circle or ring of intense light that can provide shadow less illumination and good image contrast. The experimental setup for Ring type illumination is shown in Figure 5.6. Ring lighting is a common lighting type covering a broad range of applications due to its versatility. Note that it can cause specular glare on reflective parts.

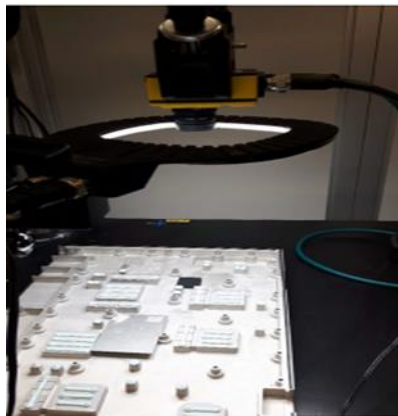


Figure 5.6: Experimental setup for Ring light illumination technique

Low angle dark field illumination experimental setup is shown in Figure 5.7. This illumination technique provides light at an extremely slight angle (10° - 15°) to the target. Features present on the surface such

as dust, scuffs or even finger prints are reflected to the camera making these surfaces appear brighter while the rest appearing darker. This lighting technique is especially good to use for surface inspection on shiny, highly reflective targets. Any height differences on the surface are highlighted.

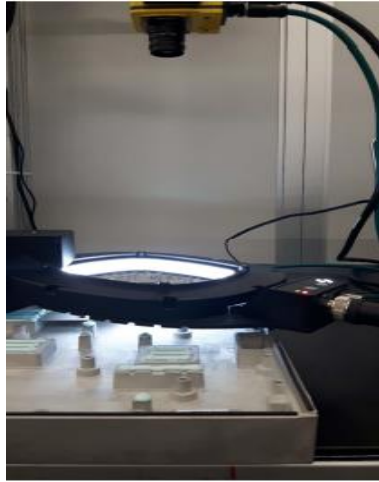


Figure 5.7: Experimental setup for Low angle dark field illumination technique

Diffuse on-axis lighting, also referred to as co-axial lighting, transmits light to the target at an angle of 90° . This illumination method highlights specular surfaces perpendicular to the camera. Surfaces at angle to the camera appear darker. This technique reduces the shadowing and has little glare. This illumination technique finds its applications in detecting flaws on shiny flat surfaces. Dome lighting illumination method provides uniform light from various angles which results in obtaining glare free images. This technique is efficient under mirrored objects as well. Dome illumination is used most often to inspect shiny, curved, or bumpy surfaces. To be effective, dome lights require proximity to the target.

5.3 Pixel Resolution Calculation

Cognex In-Sight smart camera family has models with resolutions between SVGA and 5 megapixels. In this application maximum FOV is 640x480 and height difference (WD) is 200 mm. On table above, we have pixel resolutions calculated for different camera models with focal lengths that give reasonable working distances for FOV needed. Various resolution and FOV of Cognex cameras are displayed in Table below.

Model	Pixels	Focal Length (mm)	WD (mm)	FOV (mm)	Resolution (mm/pixel)
IS7800M	800 x 600	8	1422	640 x 480	0.80
IS7800M	800 x 600	8	1622	730 x 547	0.91
IS7800M	800 x 600	6	1066	640 x 480	0.80
IS7800M	800 x 600	6	1266	760 x 570	0.95
IS7801M	1280 x 1024	12	1333	640 x 512	0.50
IS7801M	1280 x 1024	12	1533	735 x 588	0.57
IS7802M	1600 x 1200	16	1422	640 x 480	0.40
IS7802M	1600 x 1200	16	1622	729 x 547	0.45
IS7802M	1600 x 1200	12.5	1111	640 x 480	0.45
IS7802M	1600 x 1200	12.5	1311	755 x 566	0.47
IS7905M	2448 x 2048	16	1195	640 x 535	0.26
IS7905M	2448 x 2048	16	1395	747 x 624	0.31

Table 5. 1: Various resolution and FOV of Cognex derived from [32]

Precision (or repeatability) is depending mainly on lighting, positioning, image processing and analysis tools. Lighting is affecting mainly on contrast. Poor contrast will give poor repeatability. In this application we have found lighting solution that gives good contrast. Positioning is mainly influencing on precision because of optical distortion. In this application it has minor effect on repeatability. Biggest difference can be seen at same size of objects appear as different sizes in middle or at corner of an image. This can be eliminated well with image calibration. Image processing has in practice no influence in this case. We may be able to improve repeatability little by removing noise with filters. Figure 5.8 below illustrates the relationship between resolution, precision and accuracy [16].

Analysis tools has major influence, since different tools have different repeatability.



Figure 5.8: Relationship between resolution, precision and accuracy

5.4 Analysis Tool Precision

Tools to measure size and position of thermal material, tools such as blob tool and edge tool are used from the Cognex vision view software. Simplified blob tool can identify dark objects on bright background or vice versa. Blob-tool works on 1-pixel resolution. Example of blob-tool applied in this application is on right image of Figure 5.9. Edge tool can find transitions from dark to bright or vice versa. Edge tools precision depends on contrast and sharpness of an edge. Precision can be as good as $1/30^{\text{th}}$ of a pixel. In this application it probably is around $1/10^{\text{th}}$ of a pixel.

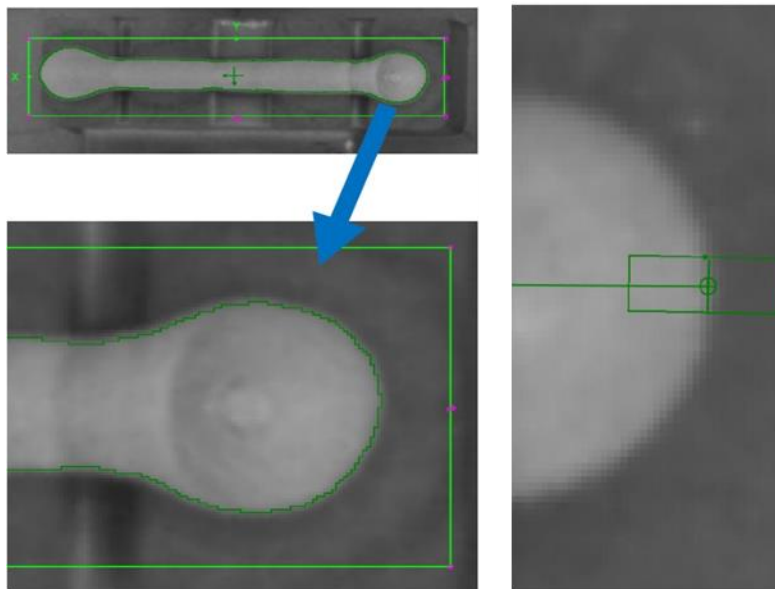


Figure 5.9: Image analysis from the Analysis Tool

First step for measurement is to find the gel beads on the product. Picture on right shows an example. As a result, we get center of mass of each blob i.e. those three crosses on each bead. Since the beads are not symmetric, center of mass is not at center of bead if measured by width and length. Therefore, edge tools need to be used to find exact width and length of a bead. See example of bead length measurement below. Cross on left side is center of mass from a blob-tool and brighter green cross on right side is exact CenterPoint measured with edge tools. Manual optical/vision inspection is meant to check and verify the correct dispensability of the machines on the products. The correct putty pattern and shape is the one which results in correct dispensed volume, uniform spreading, and uniform defined thickness over the corresponding area. Some factors to consider are pattern and size and shape of the dispensed putty.

Only lines and dots should be used for dispensing programming, so that there will be no trapped air while putty is compressed between two parts. Patterns such as circles, spirals and other closed loops are not recommended for dispensing. The pattern should be centrally located on the boss and uniformly distributed. Ericsson Supply Tallinn will use lines and dots to construct patterns with given volume.

Currently patterns are not standardized. So, each product might have bit different pattern logic (line width, gap between lines). Any irregular pattern or bended interrupted lines should be rejected.

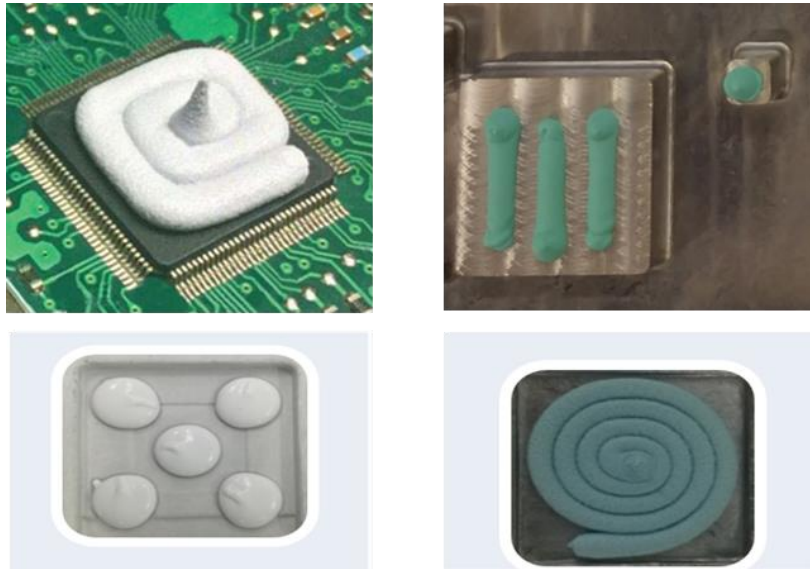


Figure 5.10: Dispersed thermal materials under various control parameters.

Size and shape of lines and dots determines whether the correct amount of putty is dispensed or not. Dispersed patterns and shapes should be compared to reference/golden sample (See 5.2). Too thin (for example, -10% from reference) and too thick lines (+10% from reference) of dispensed putty should be rejected. Any distortions in shape of lines and dots should be rejected as well. Acceptable dispensed tolerances should be defined separately for each product (even better for each area on the product), ranging from 10 to 20%.

Some examples for correct and incorrect shapes and sizes are below:

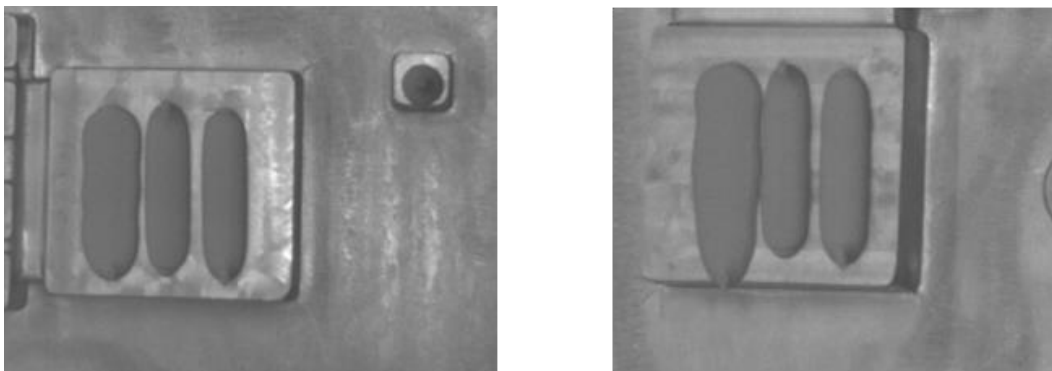


Figure 5.11: Observation of good sample and bad sample from the dispensed components

5.5 Automated Optical Inspection

Under Automated Optical Inspection the quantity of putty dispensed on the surface will be studied with the help of a 3D camera. 3D environment is needed to be transformed to 2D, because 2D AOI system will be used. For example, nominal 3mm sample line width transformed into 2D environment. Line width with 10% tolerances will change accordingly. In other words, line width should not be less than 2.85 and not more than 3.15 mm. Figure 5.12 shows the expected amount of putty quantity with tolerances.

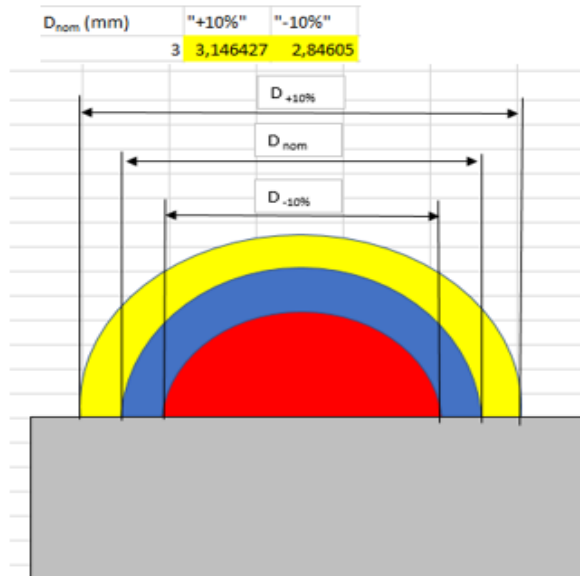


Figure 5.12: Expected thermal material quantities with tolerances

A golden sample/expected outcome will be taught to the AOI system. This is achieved by the available SOPAS engineering tool, which has the flexibility to define the parameters of the component of the line that is being studied. For instance, this component that is being studied could be a line or a dot. If it is a line, then with the help of the tool the dimensions of the desired line can be defined. Based on the target image's dimension the tool reports if the target image is within or beyond the defined dimensions. The machine vision lighting techniques contribute significantly for this study of AOI study. Several lighting conditions have been experimented. Many lighting techniques failed due to reflectivity on the surface of the radio. It was found at the end of the experiment that Darkfield lighting gives best results.

Pixel count/area tool will count in ROI specific pixels that will represent putty. For example, green in color camera and some shade of gray in monochrome image. Pattern match tool, depending on the case additional pattern match tool might be used to find similarities with the taught sample. Other tools can be used to provide better analysis and it is preferred the possibility to add Deep Learning later to the AOI system. Figure 5.2 illustrates the test setup for AOI study.

6.Results

6.1 Lighting Techniques

Different machine vision lighting techniques have been studied and the results and observations from the experiments have been presented under this section [10]. The key to the inspections system is imaging arrangement. The wavelength and form of light with respect to the DUT and camera are the most crucial elements. Extensive testing was made with direct/indirect lighting, dome lighting, coaxial lighting, brightfield lighting and darkfield lighting techniques. Wavelengths of UV, visible and near IR were also tested. Below Figure 6.1 illustrates the test setup for various lighting conditions. Different wavelengths (i.e. colors) of lighting were tested. Purpose was to find wavelength, that would give best contrast with all color combinations of mechanics and gels. It was stated earlier in Chapter 4 that the study was made under the contrast principle, and therefore the surface detail is a requirement to differentiate the thermal material from the radio surface. For this Cognex In-Sight 7905 camera has been used to capture images.

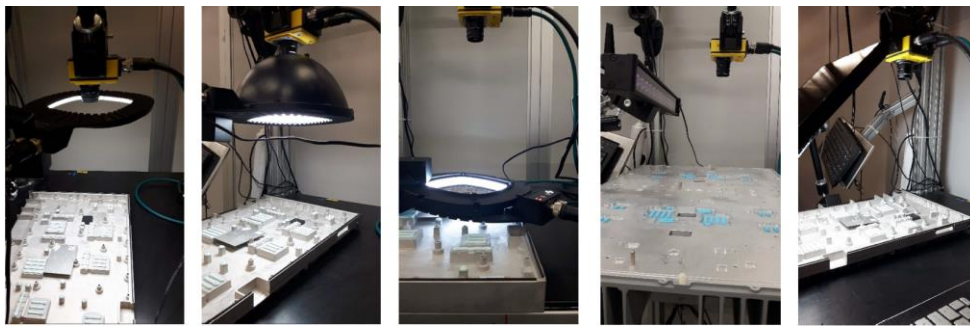


Figure 6.1: Experimental setup for various lighting conditions

Figure 6.2 illustrates the experimental setup and the captured image from Cognex In-Sight Camera for Diffused Dome lighting technique. Diffuse dome light gives disturbing reflections from shiny parts of the machined surface. The milling marks present on the surface of the radio cause disturbing reflections. These reflections can only be attenuated to a certain degree with the help Cognex Vision View software. Further attempting to distort the reflections result in loss of useful information from the image. The parameters to be evaluated are line length, line width and dot diameter. Based on the measurements and threshold values the tool returns the value interpreting if the output is within or beyond the defined criteria. Since there are random variations on mechanics surface, this lighting method is not useful. The correct thermal material pattern and shape are the ones which result in correct dispensed volume, uniform spreading and uniform defined thickness over the corresponding area. Below Figure 6.2 shows a good sample of the image observed justifying best pattern, shape and size. The most common shapes used in the factory is lines and dots to construct patterns to achieve given volume. Although the patterns are not standardized, products are expected to have different pattern logic as per their functions.



Figure 6.2: Image acquired under diffused dome lighting illumination method

Figure 6.3 shows the method for defining dimensions on an image acquired with the aid of Cognex In-Sight camera. The polygons present on the left side image is very similar to a pattern matching operation. The polygons are defined in the edit mode option of the tool and the distance between two points are identified by the camera dynamically as the camera captures the image under original scale. The right-side image on Figure 6.3 represent the identification mark by the camera. 1 denotes the camera tool has identified the presence of the edge of the defined line and 0 denotes the absence or inability of the camera tool to identify the defined dimension.

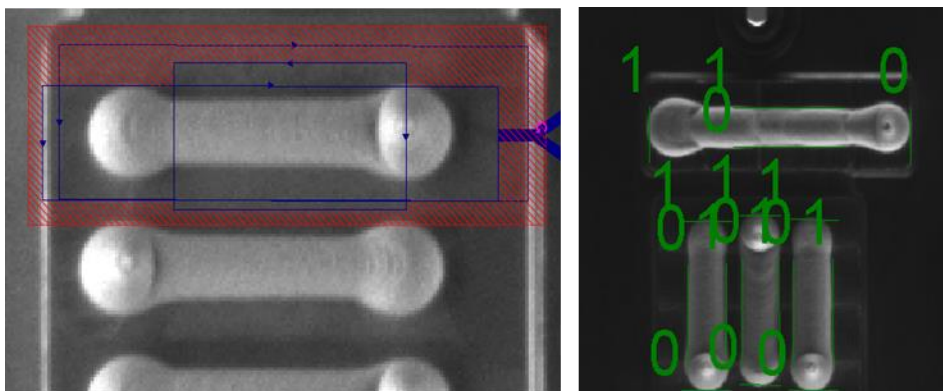


Figure 6.3: Thermal material dimension definition from the camera tool

Figure 6.4 illustrates the test setup and the image acquired with the help of Brightfield Ring lighting technique. Under Brightfield Ring-light the obtained image also gives disturbing reflections like the dome lighting technique. The reflections are caused from the shiny parts of the machined surfaces. However, this deviation is product specific and the reflections caused are variant as per products good surface finish. Due to this lighting technique is not suitable for the inspection study.



Figure 6.4: Image acquired under Brightfield illumination method

Figure 6.5 depicts the experimental setup and the image captured with the Low-angle darkfield lighting technique. The results obtained with the help of Low-angle dark field lighting is encouraging since, excellent contrast is captured between the thermal material and the radio surface. However, it can understand that this type of lighting arrangement is not suitable for such big products

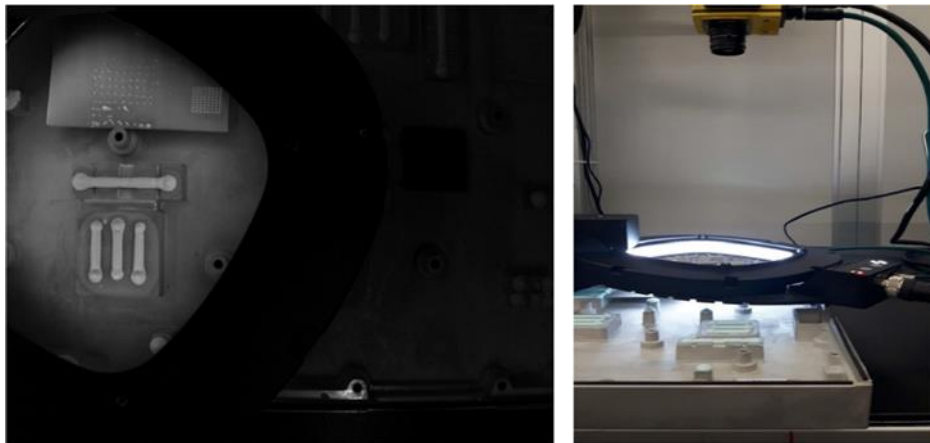


Figure 6.5: Image acquired under low-angle darkfield illumination method

Figure 6.6 illustrates the test rig setup and the image captured with Cognex In-Sight camera under Backlighting technique. Backlight used as low-angle darkfield lighting is sensitive for right distance and angle. This geometric setup also causes reflections from shiny machined surfaces. As seen from the left side of the image in Figure 6.6 the shiny reflections that are present on the surface hinder the contrast thereby, it is difficult for the tool to differentiate the thermal material and the radio surface.

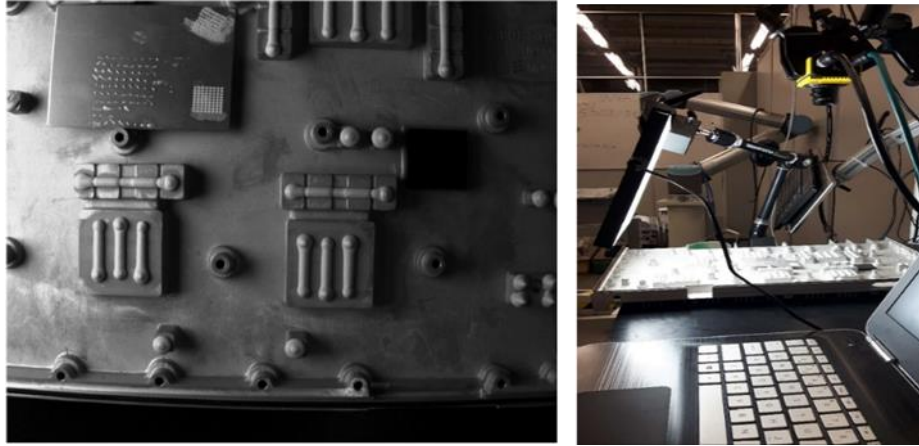


Figure 6.6: Image acquired under Backlight illumination method

Any brightfield (lighting from top) type of lighting arrangement will not work since background mechanics has large random variations in reflectivity. Darkfield lighting gives best results. Challenge is to find arrangement, where large enough area can be illuminated with 'good enough' darkfield effect. For area-based analysis with traditional vision tools target is to overexposure the gel and keep background as dark as possible – see left side of gel stripes in picture below. For 'shape based' analysis with deep learning algorithm target is to get diffuse lighting so that form of the gel is visible.

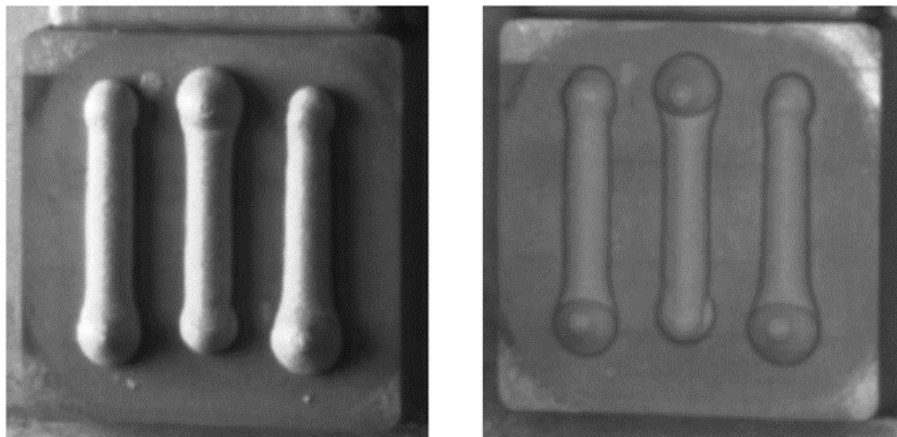


Figure 6.7: Comparison between good sample and bad sample observed during the study

6.1.1 Conclusion

Based on the study it can be concluded that and Brightfield lighting technique (lighting from top to bottom) is not suitable for the products under consideration. The primary disadvantage is the surface reflections that are caused from the machined surfaces. These machined surfaces undergo milling operation which tend to leave milling marks on the surface. These milling marks provide disturbing deviations when the surface is exposed to vision study with the help of lighting. Of all the experiments conducted the Darkfield lighting setup results are promising and gives best results. Major challenge in involving Darkfield setup is configure an arrangement where large enough area can be illuminated with the help of good enough Darkfield effect. For area-based analysis with traditional vision tools target is to overexposure the gel and keep background as dark as possible. In Figure 6.7 below, the left side of gel stripes in picture. For 'shape based' analysis with deep learning algorithm target is to get diffuse lighting so that form of the gel is visible.

6.2 Automatic Optical Inspection (AOI)

The expected outcome of the AOI is explained in detail under Automatic Optical Inspection in Chapter 6. This section outlines the results observed from attempting to implement AOI. The idea behind the study is to measure the thermal putty application parameters such as line width, line length and dot diameter of the dispensed putty on the radio surface. Since the Cognex In-Sight camera has been used for the inspection purposes, the software comes with useful tools to experiment the findings. Figure 6.8 illustrates a good sample of the image captured. Tools such as blob tool and edge tool can be used to define threshold values and draw polygons which act as limits and when the actual image is captured, the tool tries to adjust itself on top of the captured image (in here the thermal material) and displays the value of the measurements.

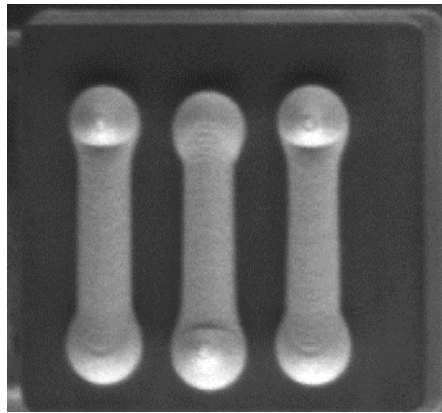


Figure 6.8: Good sample observation of the image for AOI

One of the major challenges in obtaining consistent radio surfaces which has good surface finish. This variation differs from one supplier to the other. The variation in machined appearances causes reliability problems for the AOI study. It can be understood that these variations are not controllable, because of missing appearance requirements for coating process. It is also not feasible to set such requirements because of the nature of coating processes. Variation between the supplier might result in creating separate set of models for each supplier. Some of the ideas suggested were to lower the contrast values, however, when the contrast threshold is set too low, the edge tool reports the putty missing locations as found. Thus, this measure of compensating putty chassis low contrast is not suitable. Figure 6.9 shows the Analysis made by the edge tool.

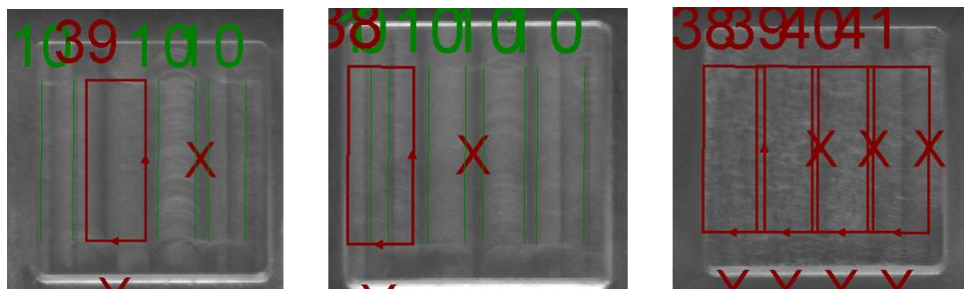


Figure 6.9: Images locating presence of milling marks on the radio surface

Another study was made to identify the radius of the dispensed putty. At times the dispensed pattern is a dot with certain quantity. It was attempted to measure the volume of the dispensed thermal material with the help of in built tools available in the Cognex Vision View software. Figure 6.10 illustrates how the polygons are defined on the tool for the camera to recognise. It is simple to create vision programs with the help of easy builder which is inside In-Sight software. Based on the image acquired by the camera, the pixel count tool reports the results. As per the defined threshold values, from the tool it can be identified if the acquired image is within the defined dimensions. It is mainly preferred for presence check and not for precision measurements. It is also not as sensitive as spreadsheet applications.

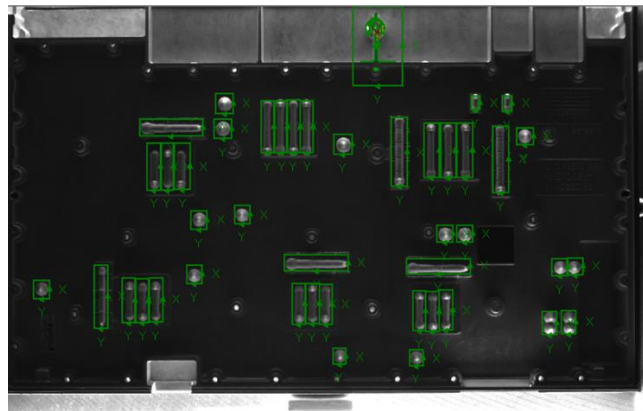


Figure 6.10: Defining measurement points using the camera tool for radius check

It is stated from the very beginning of this study that, the surface finish of this radio surfaces have an important role in successfully conducting these experiments or obtaining best results out of these experiments. The Automatic Optical Inspection is sensitive to machined surfaces and therefore does not give reliable results easily. It is also important to note that skilled and dedicated programmers are needed to create new programs and obviously skill comes with experience. To make the measurement tool work reliably, variations of the machined surfaces must be reduced. This is not the most suitable solution since the milling operation is conducted externally and its a CNC operation. Additionally, dispensing programs should be created with silent zones, however, this is also not feasible since it is not suited for all products.

6.2.1 Conclusion

As a conclusion for the AOI study, it can be stated that these products that are being studied produce varying optical results which is not a reliable measurement modality. The results produced also justify that the vision system cannot produce reliable results from that distance. Pixel counting tool used as presence check seems to be working reliably. Producing more reliable measurements would require investing additional Research and Development time and money. However, the results to be obtained are uncertain. To use high end measurements, the dispensers also needed to be programmed. The Z axis coordinate data compensation on the dispenser would be needed to reliably measure 2D dimensions. Since this implementation is looking at a possible learning algorithm, additional interfaces must be developed for statistics, which would be beneficial.

The images that are saved should not be duplicated. It is possible to be added with the help of PLC or timer delay. If not, it can be installed into automated line setup. The setup should be kept simple with camera and lights. Any changes in the setup results in reprogramming, readjustments and reconfiguration. Product variation might cause need for periodical reprogramming. The periodic reprogramming is required to define the threshold values. To efficiently handle such conditions a flexible programmer is needed. The final setup needs risk analysis for radiation hazard since the IR lights are implemented.

7. Discussion

The implemented visual guidance system for the robot are proven working effectively under standard industrial lighting condition. The radio surface, in here, the object has been detected from its relevant orientation and distance under the use of 2D camera and a laser sensor. The camera helps in capturing the x and y coordinate data herein to identify the presence of the object under its envelope. This task is achieved through pattern matching. In the SOPAS engineering tool, the desired shape has been drawn with the help of polygons. The camera when traversing above the object tries to identify this pattern and references the position. Here is where the implementation of mathematical model does the calculation for the robot manipulator to help the camera adjust and suit the described components. Monochromatic image has been used by the camera, therefore, the information to be perceived from the target has been successfully retrieved. Some of the untextured surface caused variance on the behavior of the thermal putty dispensing operation, however, this is product dependent. The working orientation for the objects has also been tested [15] [16]. Results infer that, this system is highly functional under wide perspective projection. Although the proposed method requires high end troubleshooting capabilities, its functionality is more robust than the previously conducted manual method. But the newly implemented requires less time and input for the operation. Stereo vision is argued to reach more accuracy by replacing the laser sensor that was used in here, however, for this implementation stereo vision is a little far-fetched.

Depth is of serious consideration as it is defined that the dispensing nozzle must be 3mm above the radio surface. The difficulty in selecting a suitable baseline is dealt again with the product as discussed in the existing process method section under Chapter 2. The nozzle on the robot is subjected to blocking and purging. Although these factors were discussed exclusively under the control parameters in Chapter 6, this timely issue can be overcome by continuous operation. One of the many constraints for continuous operation is the products deviation from its original defined location. This deviation could be due to external factors. Under such condition the dispensing takes place at wrong locations or angles and this causes an interrupt to the operation [22]. The system must be calibrated again thereby introducing the dispensing points again. This problem of deviation of the product from the original position can be overcome with the introduction of an algorithm which tends to learn the deviations caused and thereby account the offsets and continue the dispensing operation. The workaround for such learning algorithm is briefly discussed under future work section.

An inspection study was also conducted attempting to quantify the volume of thermal material that is being dispensed on the radio surface. For this a Cognex In-Sight smart camera has been used to capture images of the radio surface with dispensed gel under various lighting conditions. The Automatic Optical Inspection (AOI) results infer that mostly due to milling marks present on the surface of the radio, the camera is not able to identify the thermal material and thereby the software gives failed results. Simple way to create vision programs is possible via Easybuilder (inside Insight program). Based on observation, pixel count tool will give best results. It is mainly for presence check, not precision measurements. It is not as sensitive to variations as Spreadsheet application. It was proposed to make measurement tools work more reliably variation of machining shall be heavily reduced. However, this proposition does not

seem practical. Another suggestion was to create a dispensing program with silent zones which is not possible in all products [32].

The overview of the system architecture consists of a dispensing nozzle which takes the role of an end effector, a GRACO dynamite extruder system to pump the thermal interface material to the nozzle. The nozzle is controlled by a valve system which controls the opening and closing of the nozzle through-put. The complete structure of this system is elaborated under Chapter 5. The reference points are calculated by the addition of current coordinates in TCP coordinate frame and the transformation brings the current pattern on the camera to the desired pattern defined in the SOPAS tool. The motivation selecting this process to automate was the organization's growing demand in smart manufacturing concepts. The work has been established with the intention of introducing more intelligence to the robot system, that is by deploying a learning algorithm which can isolate the visual component after the initial referencing of the target. Compared to conventional pick and place task, this process automation technique requires extensive mathematical simplification. Without resolving the mathematical model, it is practically impossible to account the varying z coordinate data. The x and y coordinate data can be extracted from the pattern matching from the 2D camera, but the z coordinate information can only be extracted with the help of a laser sensor. These sensors can be used alone or together with a sensory data to obtain the position information of the target [23]. Additionally, different vision sensors can be used to obtain different sensory data. For instance, instead of using SICK PIM60, it is proposed to study the operation under Cognex IS 7905 cameras. This is due to Cognex camera's better resolution and fast processing capabilities. Another approach would be to place the camera under different configurations. The current implementation has eye-in-hand configuration, whereas eye-to-hand or redundant configurations can also be considered.

As clearly stated in the motivation, the primary attempt of this thesis work is to automate the process task by bringing practical approaches. While implementing this process, the ease of troubleshooting was also considered as requirement for high end knowledge would be a disadvantage for a line of business whose business is not automation. Robustness is related to reliability. If a system is more robust it means that it can work several different conditions. It is not suitable to define under which conditions the system works precisely. But throughout the tasks, some work contributes to the increase in robustness. The implemented mathematical model seems to be efficient to any product that arrives for dispensing. The controller structure is easy to adhere for modifications and desired programming. The meaning of the parameters and implementation is also easy to understand for programmers who are not experts in the field of robotics and machine vision.

8.Summary

8.1 Summary (English)

In this thesis work, a vision guidance system has been designed with the motivation of automating the thermal putty dispensing operation at ERICSSON EESTI AS. The work began with an alternate proposal for now existing manually dispensed thermal putty operation. A mathematical model has been developed to ease the robotic manipulation. Four points on the surface of the product has been used as reference including the origin. A laser sensor has been used to extract the z coordinate data. SICK PIM60 camera has been used for object recognition and the volumetric analysis study has been conducted for inspection purposes.

The results of the volumetric study have been disclosed and concluded that the use of 3D camera is not suitable for such products. This mainly due the milling marks present on the chassis of the radio surface. The system is designed in such a way that when the product arrives to the robot, the camera indexes the reference points on the radio surface looking for a predefined reference image and simultaneously extracting z coordinate data. The final integration of the system involves GRACO Dynamite Extruder which pumps the putty to a high-pressure valve and a pneumatic valve regulator. Fewer test runs have been successfully conducted.

8.2 Summary (Estonian)

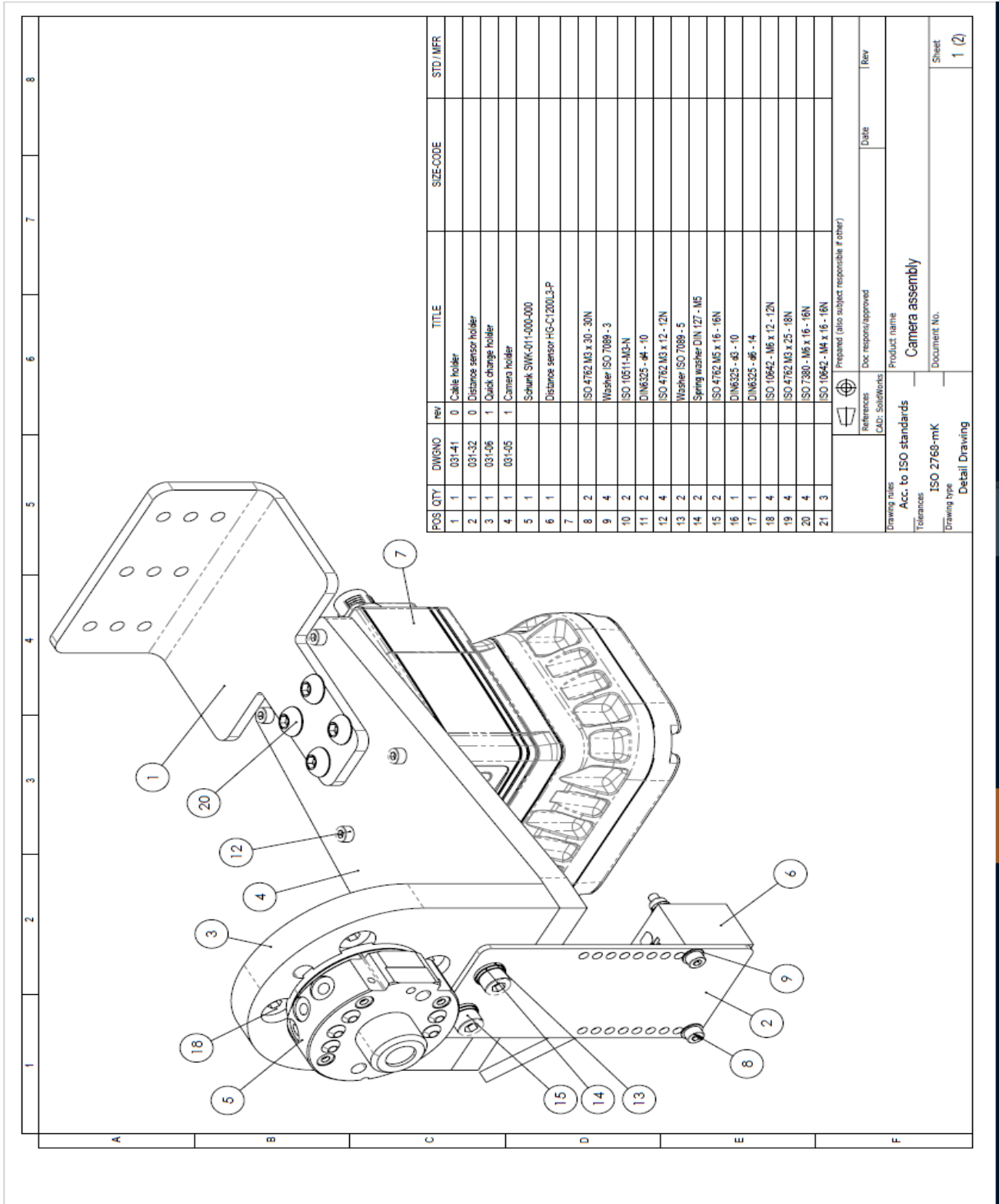
Selles lõputöös projekteeriti nägemisjuhtimissüsteem, et automatiseerida termopasta määrimise operatsiooni Ericsson Eesti AS's. Töö algab alternatiivide pakkumistega, kuidas olemasolevat manuaalset termopasta määrimist arendada. Matemaatiline mudel on arendatud, et kergendada roboti manipuleerimist. Neli punkti toote tasapinnal on kasutatud seose loomiseks, sealhulgas orginaaltasapinda. Laseri sensorit on kasutatud, et z oordinaadi andmeid oleks võimalik välja võtta. SICK PIM60 kaamerat on kasutatud objekti tuvastamiseks ja kaamerat on kasutatud, et uurida mahulisi analüüse. Mahuliste analüüside tulemusena on uuring lõpetatud ja järeltatud, et 3D kaamera ei ole mõeldud selliste toodete jaoks. Seda eelkõige sellepärast, et frees märke on märgata radiaatorite pindadel. Süsteem on disainitud sedaviisi, et kui toode jõuab roboti alla, kaamera tuvastab tasapinna punkte radiaatoril, otsides eelnevalt kindlaksmääratud võrdluskujutisi ja samaaegselt z-koordinaatandmeid. Süsteemi viimane integreerimine hõlmab GRACO Dymamite ekstruuderit, mis pumpab termopastat kõrgel rõhul ventiilist välja. Vähem katseid on edukalt läbi viidud.

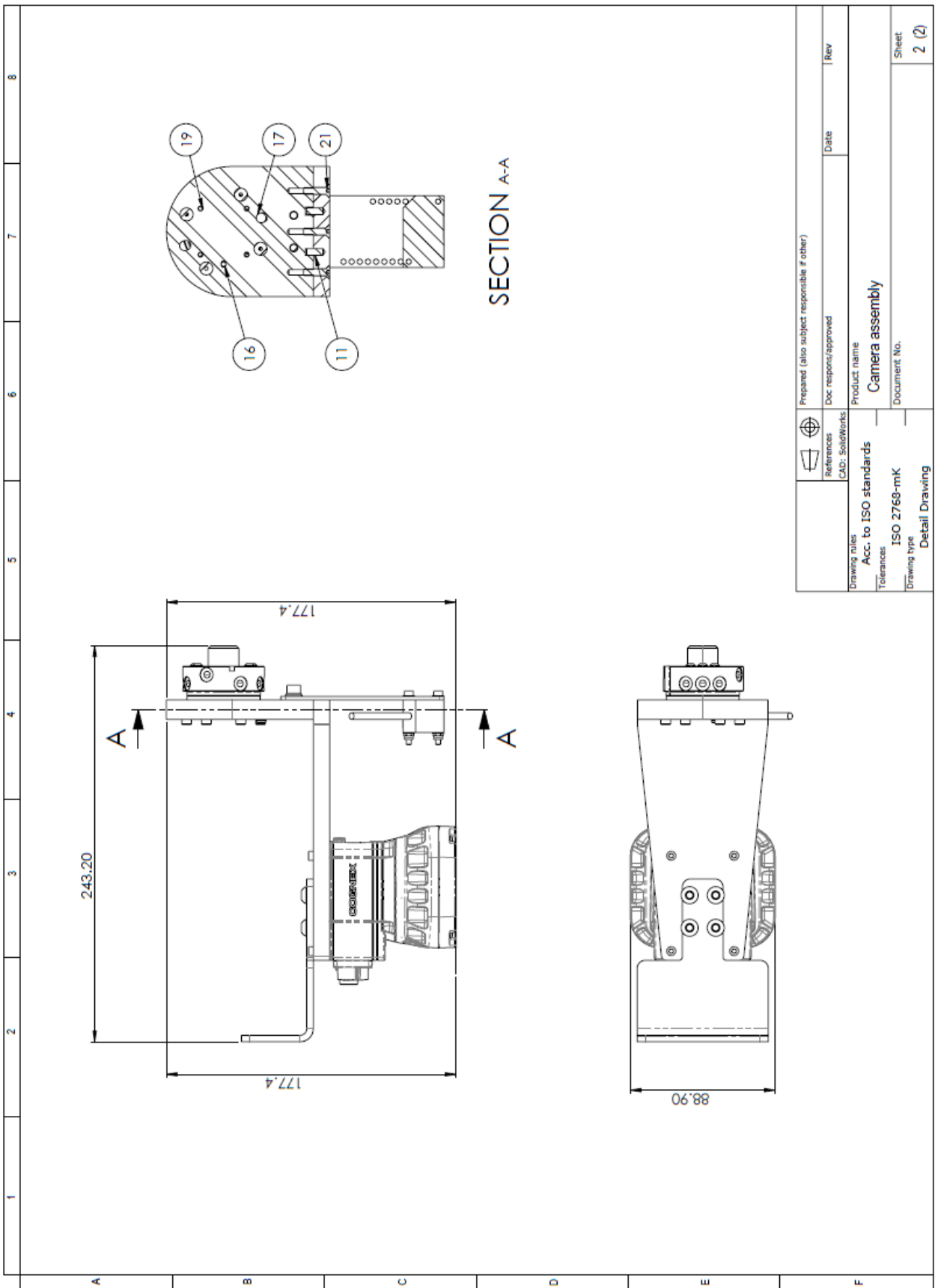
Bibliography

- [1] L. Brown, Steven & Pierson, Harry & Parnell, Gregory. (2017). An Operations Management Perspective on Collaborative Robotics.
- [2] Thomas Solund. (2016). Towards Plug-n-Play robot guidance: Advances 3D estimation and pose estimation in Robotic applications.
- [3] Jordi Viver Escale. (2015). Human-robot interaction in the industry.
- [4] Sven Behnke, Maren Bennewitz. (2017). Motion Planning Strategy For a 6-DOFs Robotic Arm In a Controlled Environment
- [5] M.R. de Gier. (2015). Control of a robotic arm: Application to on-surface 3D-printing.
- [6] Johannes Schrimpf. (2013). Sensor-based Real-time Control of Industrial Robots.
- [7] Jessica Garcia Castano. (2018). Implementation of collaborative robots in an assembly line.
- [8] Burak Dogan. (2010). Development of a Two-fingered and a Four-fingered robotic gripper.
- [9] Swagat Kumar, Anima Majumder, Samrat Dutta, Sharath Jotawar, Ashish Kumar, Manish Soni, Venkat Raju, Olyvia Kundu, Ehtesham Hassan, Laxidhar Behera, K.S. Venkatesh, Rajesh Sinha. (2017). Design and Development of an automated Robotic Pick & Stow System for an e-Commerce Warehouse.
- [10] Joni Sipponen. (2010). Employing Machine Vision to a Manufacturing Line.
- [11] Roger Bostelman. (2018). Performance measurement of mobile manipulators.
- [12] Seyed Sadegh Mohammadi. (2011). Computer vision for autonomous mobile robotic applications.
- [13] Carlos Gil Camacho. (2016). Part Detection in Online-Reconstructed 3D Models.
- [14] Merritt Jeckins. (2017). Detecting and Grasping Sorghum Stalks in Outdoor Occluded Environments.
- [15] C. Schletter, E. Guiffo Kaigom, M. Priggemeyer, D. Losch, G. Grinshpun, R. Waspe, J. Rossmann, B. Ridge, M. Tamosiunaite. (2016). A Reconfigurable robot workcell for fast set-up of automated assembly processes in SMEs.
- [16] Tarmo Rouhiainen. (2015). Automated Optical Inspection in Automotive Assembly Line.

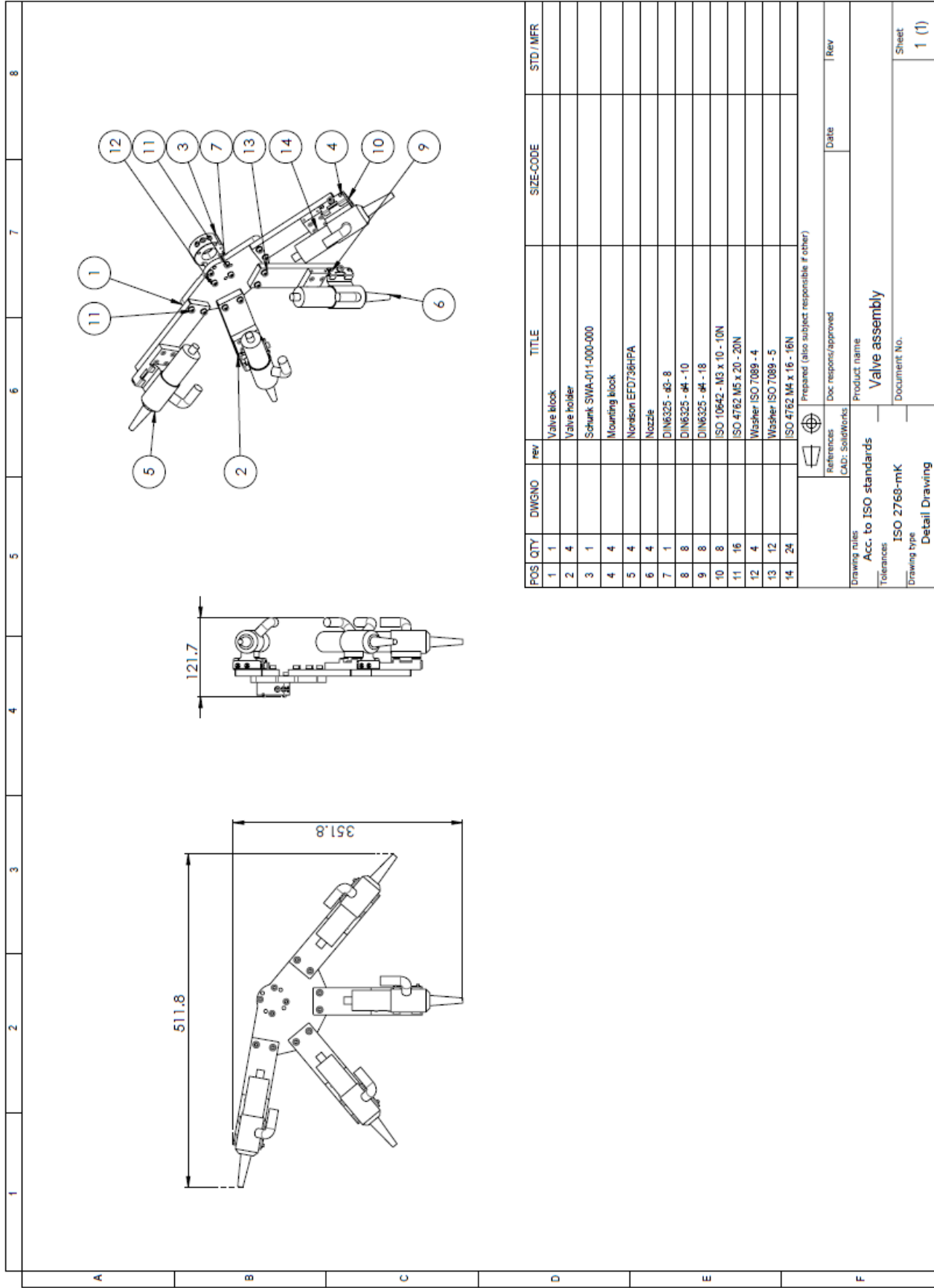
- [17] Venkateshwara Mehha. (2018). Automated Tool Path Planning for Industrial robots in material handling.
- [18] S. Wade-McCue, N. Kelly-Boxall, M. McTaggart, D. Morrison, A.W. Tow, J. Erskine, R. Grinover¹, A. Gurman, T. Hunn, D. Lee, A. Milan, T. Pham, G. Rallos, A. Razjigaev, T. Rowntree, R. Smith, K. Vijay, Z. Zhuang, C. Lehnert, I. Reid, P. Corke, and J. Leitner. (2018). Design of a Multi-Modal End-Effector and Grasping System.
- [19] Manuel Goncalo Soares Correira Vieira de Sousa. (2016). Manufacturing of aerospace composite material parts using collaborative robots.
- [20] Investigation of Heat Sink Efficiency for Electronic Component Cooling Applications (2014) Z. Staliulionis, Z. Zhang, R. Pittini, M. A. E. Andersen, P. Tarvydas, A. Noreika
- [21] Labudzki, Remigiusz & Legutko, Stanislaw & Raos, Pero. (2014). The essence and applications of machine vision. Tehnicki Vjesnik. 21. 903-909.
- [22] Rainer Bischoff and Volker Graefe. (1998). Machine Vision for Intelligent Robots.
- [23] Golnabi, H. Asadpour, A. (2007). Design and application of industrial machine vision systems Robotics and Computer-Integrated Manufacturing. 630– 637.
- [24] Lee, W. Jeon, C. Hwang, C. (2008). Implementation of the machine vision system of inspecting nozzle. 3rd Int. Conf. on Convergence and Hybrid Information Technology, Busan (Korea), 11-13.
- [25] Vickers, J. (2008). Illumination: Getting the Basic Right. First Sight Vision Ltd, Surrey.
- [26] Wang, M Wei, J. Yuan, J, Xu, (2008). Research for intelligent cotton-picking robot based on machine vision. Int. Conf. on Information and Automation, Zhangjiajie (China) 800-803.
- [27] <https://www.universal-robots.com/> [Accessed: 01/03/2019]
- [28] <https://www.sick.com/> [Accessed: 10/03/2019]
- [29] <https://www.panasonic-electric-works.com/> [Accessed: 12/03/2019]
- [30] <https://www.nordson.com/> [Accessed: 25/03/2019]
- [31] <https://www.graco.com/> [Accessed: 28/03/2019]
- [32] <https://www.cognex.com/> [Accessed: 28/03/2019]

Appendix Appendix A





Prepared (also subject responsible if other)		Date	Rev
References	Doc. respons/approved		
CAD: SolidWorks	Product name		
Camera assembly			
Drawing rules	Document No.		
Acc. to ISO standards			
Tolerances	ISO 2768-mK		
Drawing type	Detail Drawing		
			Sheet
			2 (2)



POS	QTY	DWGNO	REV	TITLE	SIZE-CODE	STD / MFR
1	1			Valve block		
2	4			Valve holder		
3	1			Schunk SWA-011-000-000		
4	4			Mounting block		
5	4			Nordson EFD736HPA		
6	4			Nozzle		
7	1			DIN6325 - a6- 8		
8	8			DIN6325 - a4 - 10		
9	8			DIN6325 - a4 - 18		
10	8			ISO 10642 - M3 x 10 - 10N		
11	16			ISO 4762 MS x 20 - 20N		
12	4			Washer ISO 7089 - 4		
13	12			Washer ISO 7089 - 5		
14	24			ISO 4762 M4 x 16 - 16N		

Prepared (also subject responsible if other)

References:
 Doc: resp/ons/approved
 CAD: SolidWorks

Date: _____ Rev: _____

Drawing rules:
 Acc. to ISO standards

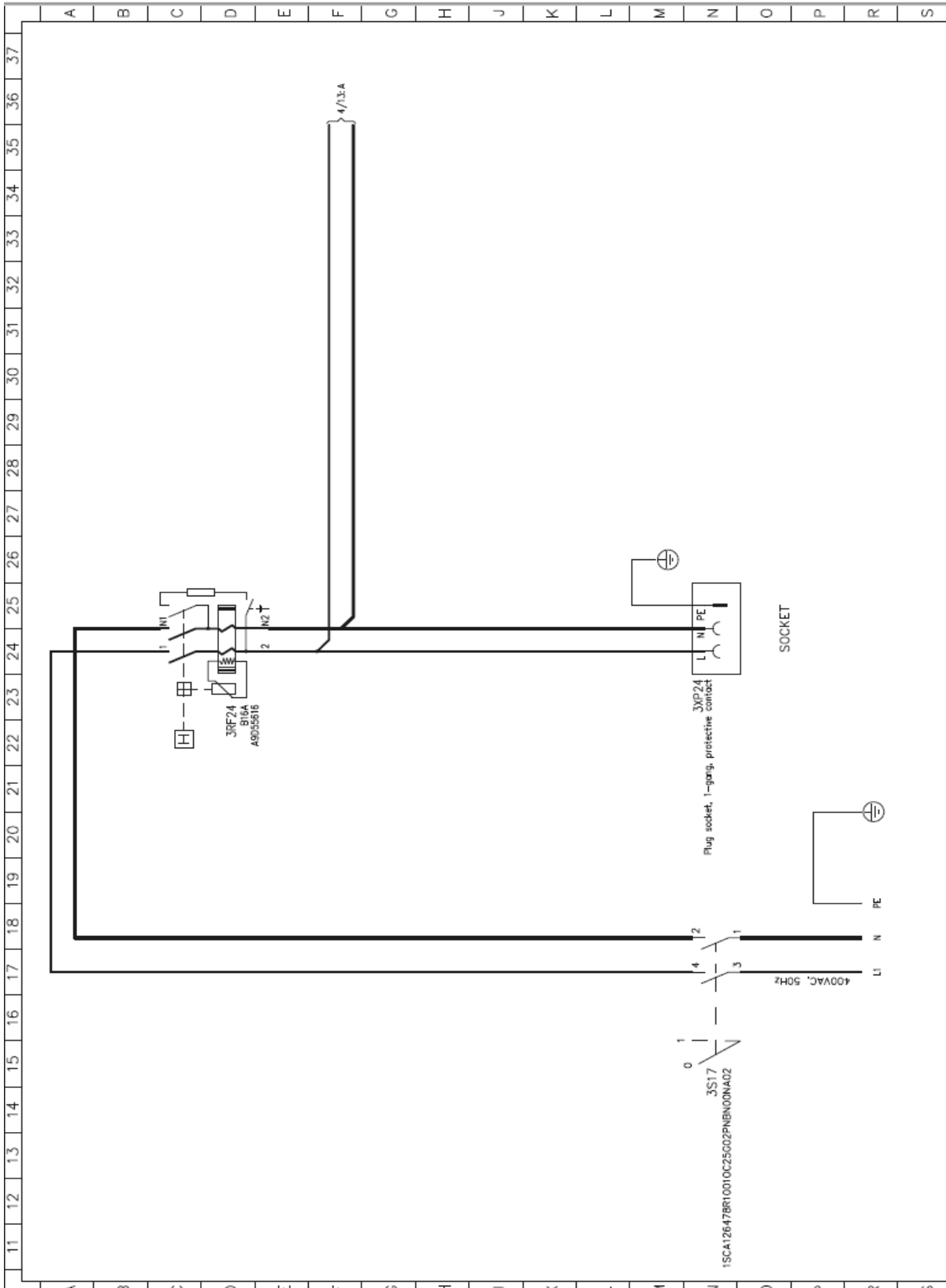
Tolerances:
 ISO 2768-mK

Drawing type:
 Detail Drawing

Product name:
 Valve assembly

Document No.:

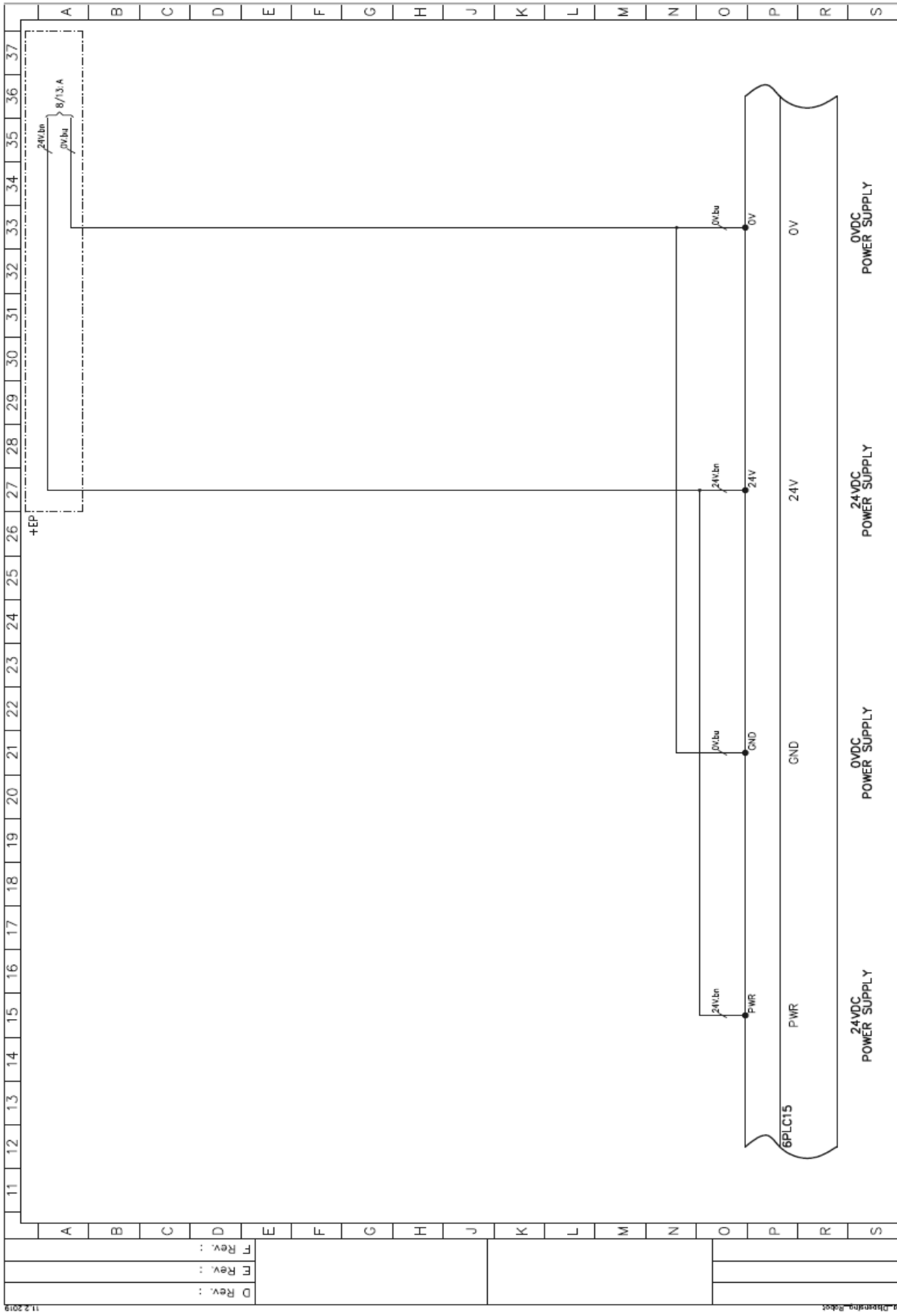
Sheet:
 1 (1)



Plan.	Object ID	Electrical position	Job no.
Draw.	Sheet	+HMI	
Check	Drawing no.		

MAIN POWER SOCKETS

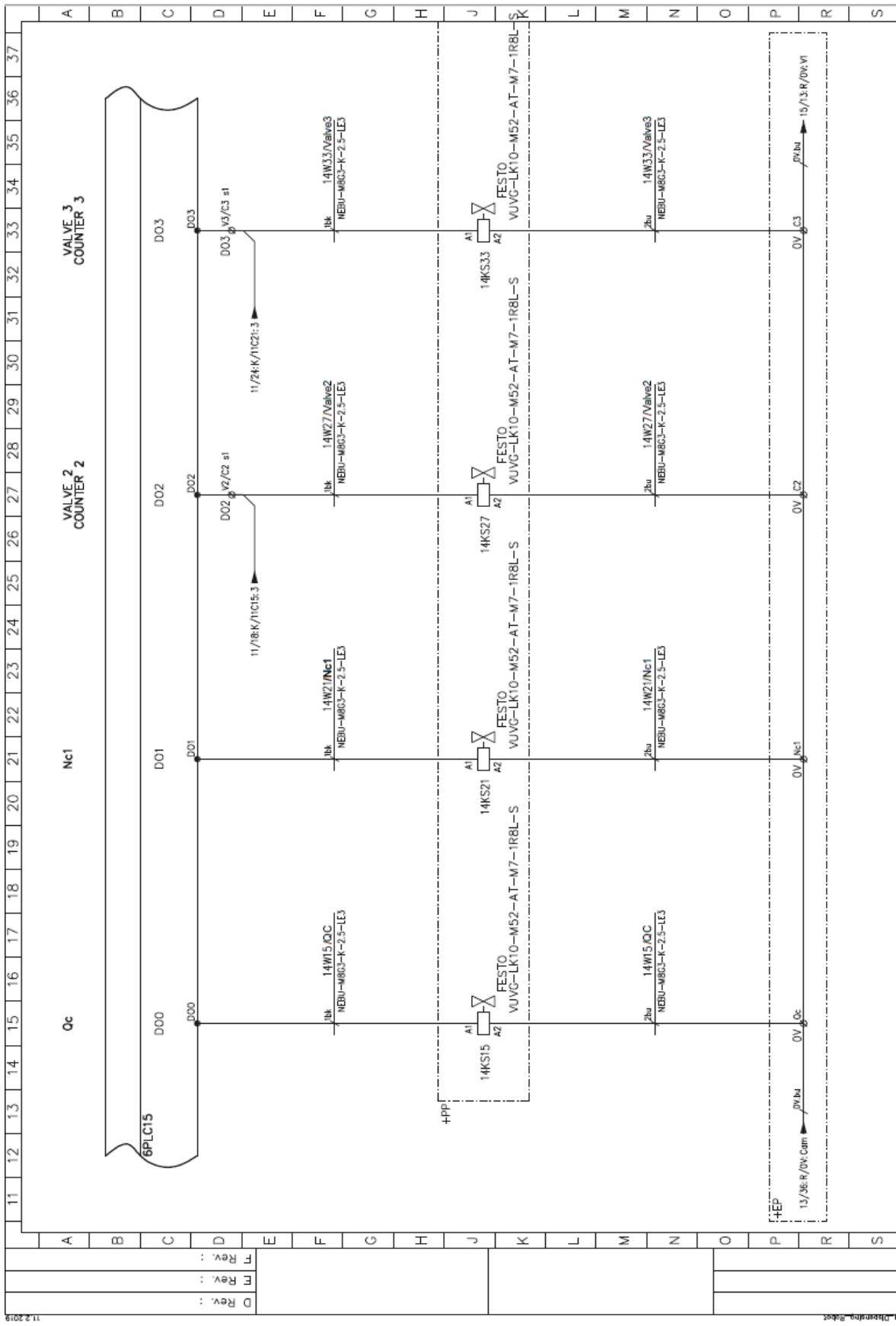
A Rev. :	
B Rev. :	
C Rev. :	
D Rev. :	
E Rev. :	
F Rev. :	



A Rev. :											ROBOTS I/O											Job no.										
B Rev. :											Sheet											Drawing no.										
C Rev. :											Electrical position											+UR.10e										
D Rev. :											Plan.											Subject ID										
E Rev. :											Draw.											Sheet										
F Rev. :											Check											Drawing no.										

11.2.2019

181001 - Large Area Drawing - Sheet



A Rev. :		ROBOTS I/O		Job no.	
B Rev. :				Electrical position	
C Rev. :				+EUR_10e	
		Object ID		Drawing no.	
		Plan.		Sheet	
		Draw.		Check	
		Check			

